A NOVEL ANIMAL MODEL OF SOMATOSENSORY-EVOKED REFLEX SEIZURES INDUCED BY PERIPHERAL STIMULATION

Abbreviated title: A novel animal model of somatosensory-evoked reflex seizures

Aleksandra Bortel, Roland Pilgram, Ze Shan Yao, Amir Shmuel

Montreal Neurological Institute, McConnel Brain Imaging Centre
Departments of Neurology and Neurosurgery and Biomedical Engineering
McGill University, Montreal, QC, H3A 2B4, Canada

Correspondence to:
Aleksandra Bortel or Amir Shmuel
3801 University, room NW255
Montreal, QC, Canada H3A 2B4
Tel: +1-514-398-5943
Fax: +1-514-398-8106
E-mail: aleksandra.bortel@mcgill.ca, amir.shmuel@mcgill.ca

Keywords: animal model of seizures; reflex seizures; epileptic discharges; somatosensory stimulation; primary somatosensory cortex; S1FL; S1 forelimb; high frequency oscillations

Acknowledgements:

This study was supported by the Canadian Institute of Health Research (Grant MOP-102599) and the Natural Sciences and Engineering Research Council of Canada (RGPIN 375457-09 and RGPIN 2015-05103) awarded to A.S. We thank Jean Gotman, Victor Mocanu and Pascal Kropf for their helpful technical advice and discussions. We thank Laura Diamond and Katie Hu for scientific English editing.

ABSTRACT

Methods for eliciting epilepsy in animal models induce seizures in large parts of the brain or damage the brain. Here we introduce a novel animal model for generating focal somatosensory-evoked reflex seizures non-invasively without causing damage to the brain. Specifically, we electrically stimulated digits or forepaws of adult rats sedated with dexmedetomidine and measured neurophysiological activity using laminar probes inserted in the forelimb representation of somatosensory area S1.

We observed seizures generated during the electrical stimulation period with prolonged discharges following cessation of the stimulus. Electrical stimulation of the forepaw elicited more seizures than stimulation of a digit. The neurophysiological activity during the seizures showed higher amplitudes than during normal evoked responses. High-frequency oscillations were observed prior to and during the seizures, with amplitudes higher than those associated with normal evoked responses. Seizures were typically followed by refractory periods in which both spontaneous activity and evoked responses showed lower amplitudes relative to their amplitudes prior to the seizures. Similar seizures were recorded by Electrocorticography arrays placed over the dura matter, strongly indicating that the seizures were not induced by cortical damage caused by the insertion of the probes. Using optical imaging of cerebral blood volume, we observed that the initially generated seizures were focal and confined to the forelimb representation in area S1. However, these seizures propagated from the onset zone to a larger territory, not only during the electrical stimulation period but also following its cessation. Finally, unlike rats sedated with dexmedetomidine, rats anesthetized with urethane showed no ictal discharges, strongly indicating that seizure generation depended on the dexmedetomidine.

Our proposed animal model generates seizures evoked by sensory-electrical stimulation free of artifacts or brain damage. Our model can be used for studying the mechanisms underlying the generation and propagation of reflex seizures, and for evaluating the efficacy of antiepileptic drugs.

SIGNIFICANCE STATEMENT

Inducing seizures in animal models by applying non-spatially-specific electroshock or systemic administration of convulsants causes non-focal seizures and – in the case of electroshock – damage to the brain. While invasive, focal-administration of convulsants or electrostimulation directly to the brain can induce focal seizures, these methods often cause brain damage. Here we introduce a novel animal model of somatosensory-evoked reflex seizures triggered by peripheral stimulation. Induced seizures are brief and artifact-free, with no direct application of convulsants or direct electrostimulation. Consequently, their induction does not damage the brain. The elicited seizures are focal at onset and propagate following the onset. Our proposed animal model can be used for studying the laminar-specific mechanisms underlying the generation and propagation of seizures, and for evaluating the efficacy of antiepileptic drugs.

INTRODUCTION

Reflex seizures are seizures elicited by specific sensory stimulation. These seizures may be triggered by various types of stimuli that are patient-specific (Guerrini et al., 1992; Striano et al., 1992; Panayiotopoulos, 2005; Striano et al., 2012; Sala-Padro et al., 2015; Wolf, 2015). In humans, reflex seizures can be induced by simple somatosensory stimulation, such as a cutaneous sensorial stimulus (Loscher, 1999; Sarkisian, 2001; Suzuki et al., 2015; Wolf, 2015; Koepp et al., 2016; Arican et al., 2017). Touch-based somatosensory-evoked seizures, termed Touch Induced Seizures (TIS), are associated with cortical hyper-excitability and are classified as reflex seizures induced by a simple stimulus (Striano et al., 2012; Sala-Padro et al., 2015; Wolf, 2015). In humans, TIS can be evoked by specific movements such as skin friction, touching, tapping, tooth brushing, or stimulation of the external ear canal (Striano et al., 2012; Italiano et al., 2014). Electrical stimulation of peripheral nerves can also induce somatosensory-evoked seizures (Deonna, 1998). Usually, TIS are focal seizures with no impairment of consciousness (Deonna,

1998; Striano et al., 2012; Sala-Padro et al., 2015) and may have only electrographic display without any overt clinical manifestations (Panayiotopoulos, 2005).

To date, only genetically modified epilepsy-prone species have been described as models for studying photosensitive and audiogenic reflex seizures (Sarkisian, 2001; Kandratavicius et al., 2014; Italiano et al., 2016). Current animal models that are seizure-susceptible in response to photic and/or audiogenic stimulation include the photosensitive baboon (Papio papio), the audiogenic epilepsy prone rat (GEPR) and DBA/2 mice (Sarkisian, 2001; Kandratavicius et al., 2014). However, to date, no animal model has been introduced for inducing seizures by peripheral somatosensory stimulation. Here we introduce a novel animal model of somatosensory-evoked reflex seizures induced by electrical peripheral somatosensory stimulation, without direct application of electrical current or convulsant to the brain.

Electrical stimulation or administration of chemical compounds including pentylenetetrazol, tetanus toxin, and penicillin have been used to elicit seizures in animal models for many years (Sarkisian, 2001; Engel, 2004; Kandratavicius et al., 2014). However, these techniques bear several disadvantages. For instance, a commonly used electrical stimulation technique for inducing acute seizures, termed *electroshock-induced seizures*, modifies activity in the larger part of the brain and thus, the induced seizures are not focal. Moreover, all electrical stimulation techniques used to induce seizures cause electrical artifacts that interfere with studying the spatiotemporal dynamics of neuronal activity. They also cause damage to the brain by eliciting inflammation, activation of glial cells, and disruption of the blood-brain barrier (van Violet and Gorter, 2017). Chemical injections into the brain lack spatiotemporal precision and cause neuronal damage and reactive gliosis (Osawa et al., 2013). This motivates the introduction herein of a novel, artifact-free model of seizures in adult rats evoked by peripheral somatosensory stimulation of a digit or forepaw.

Seizure symptoms of epilepsy are often associated with highly-modified cortical activity. Indeed, seizures induced by direct application of chemo-convulsants to rat brain slices lead to permanent changes in the somatosensory representation of the cortex (Borbely et al., 2006). Similarly, *in vivo* direct intracranial electrical stimulation of the rat corpus callosum and neocortex causes seizures and substantially modifies activity in the sensorimotor cortex (Ozen et al., 2008; Flynn et al., 2010; Vuong et al., 2011). Furthermore, experiments performed on rodent brain slices demonstrate that seizure characteristics are determined by distinct laminar distributions of different cell types and their intra- and inter-laminar excitatory and inhibitory connections (Yang and Benardo, 1998,

2002; Borbely et al., 2006). Seizures induced in brain slices by applying the chemo-convulsant 4-aminopyridine show that each laminar network contains cell assemblies that may work as a discharge initiator (Barkai et al., 1995; Yang and Benardo, 2002). The same chemo-convulsant, 4-aminopyridine, infused *in vivo* to the deep layers of rat primary somatosensory cortex reduces cross-laminar Local-Field Potential (LFP) synchrony during recurrent focal seizures (Harris et al., 2018). Accordingly, our model provides the opportunity to study the spatiotemporal mechanisms underlying the onset, propagation, and termination of epileptic activity in a layer-specific manner. Changes in LFP frequency bands lower than 70 Hz are informative for seizure description and prediction (Modur et al., 2011). In addition, low-voltage rapid discharges with frequencies within the gamma band (30–100 Hz) can often be observed at seizure onset zones (Wendling et al., 2002). Furthermore, high-frequency oscillations (HFOs) termed ripples (80-200 Hz) and fast ripples (250-600 Hz), facilitate synaptic transmission through local networks (Staba, 2012). Interestingly, in epileptic patients and animals, the power of pathological HFOs increase before seizure initiation (Jacobs et al., 2009; Modur et al., 2011; Staba, 2012). Therefore, HFOs may serve as biomarkers of epileptogenic neural networks and predictors of seizure occurrence (Jefferys et al., 2012).

Here we demonstrate the induction of seizures in adult rats by peripheral electrical somatosensory stimulation of the digits or forepaw. To this end, we applied simultaneous intrinsic optical imaging and neurophysiological recordings. We specify the characteristics of the ictal discharges, and we analyze the conditions required to elicit them. We present the seizures' spatial extent relative to normal sensory responses to peripheral electrical stimulation in cortical area S1FL. Our study introduces an artifact-free animal model of somatosensory evoked reflex seizures.

MATERIALS AND METHODS

Animals and surgical procedures

All procedures were approved by the animal care committees of the Montreal Neurological Institute and McGill University, and were carried out in accordance with the guidelines of the Canadian Council on Animal Care. Experiments were performed on 35 adult (67-107 day old) male Sprague–Dawley rats weighing 300–580g. The rats were housed under controlled environmental conditions at 22±2º C with a 12h light/12h dark cycle (lights on from 7:00 a.m. to 7:00 p.m.) and received food and water ad libitum.

The rats were initially anesthetised with a solution of Xylazine (10mg/kg i.p.; Bayer Inc., Canada) and Ketamine (50mg/kg i.p.; Wyeth, Canada). They were then intubated and placed in a stereotaxic frame. The surgical procedure was performed under anaesthesia with isoflurane (0.6-2%; Benson Medical Industries Inc., Canada). During the surgery, the rats were ventilated with a mixture of oxygen (50%) and medical air (50%). Physiological parameters, including temperature, heart rate, and PaO2 measured with pulse oximetry, were monitored continuously. The scalp was incised to expose the skull covering the primary somatosensory cortex (S1) of the left hemisphere. One stainless steel screw (2.4 mm in length) was fixed to the skull above the visual cortex of the right hemisphere and was used as a ground and reference. The area of skull overlying S1 was thinned until soft and transparent. We then performed an approximately 4 mm wide square-shaped craniotomy, centered on the forelimb representation in area S1 (S1FL) based on a stereotaxic atlas (AP 0.00 mm, ML ±4.50 mm, DV –2.5 mm; (Paxinos and Watson, 2005). The dura was resected and a linear multi-electrode probe was inserted into area S1FL. At the end of the surgical procedure, a silicon chamber was created around the craniotomy and filled with Hank's Balanced Salt Solution (Invitrogen, Canada). Following the surgery, prior to starting the recordings, we switched to ventilating with a mixture of 20% oxygen and 80% medical air. At the same time, we injected a single dose of buprenorphine (0.04 mg/kg, s.c.; Schering-Plough, UK) and started administration of dexmedetomidine (0.075 mg/kg/h, s.c.; Pfizer Inc., Canada) that remained continuous throughout the recordings. To examine the effect of the anesthesia on the epileptic activity, we injected six animals with a single dose of urethane (1.2 g/kg, i.p.; Sigma-Aldrich, Canada) instead of administering dexmedetomidine and buprenorphine. Isoflurane administration was stopped following the administration of either dexmedetomidine and buprenorphine, or urethane.

Electrical stimulation of a single digit or forepaw

Electrical stimuli were delivered to the right D3 digit, D5 digit, or forepaw using a stimulator-isolator (A365, WPI, Sarasota, FL). For digit stimulation, we attached two electrodes (anode and cathode; PlasticsOne, Roanoke, VA) per digit, one on each opposing side of the digit. For forepaw stimulation, we inserted needle electrodes into the web spaces of digits 2/3 and 4/5 of the right forepaw.

We began our experiments by optical imaging of area S1FL in order to guide the insertion of the neurophysiology probe to the responding region. Stimulation runs for eliciting cerebral blood volume (CBV) based optical imaging responses (Figure 1) consisted of ten 12s-long trials, separated by inter-trial intervals of 12s during which no stimulus was delivered. Each stimulation trial began with 2s recordings of baseline activity, followed by 4s of stimulation and 6s of baseline activity. The 4s stimulus consisted of a train of electrical pulses delivered to D3, D5, or the forepaw at a frequency of 8 Hz. The stimulus intensity was 1-1.5 mA and the duration of each single electrical pulse was 1ms. The polarity of stimulation was switched in each pulse relative to the polarity in the preceding pulse.

Eight timulation runs for inducing seizures were performed in each of the rats. These stimulation runs consisted of ten 35s-long stimulation trials, separated by ten 35s-long trials in which no stimulus was delivered (see time-courses in Figure 11A and 12A). Each stimulation trial started with 5s recordings of baseline activity, followed by 10s of stimulation and 20s of baseline activity. The 10s stimulus consisted of a train of electrical pulses delivered to D3, D5, or the forepaw at a frequency of 8 Hz. The stimulus intensity was 2 mA and the duration of each single electrical pulse was 1ms. The polarity of stimulation was switched in each pulse relative to the polarity of the preceding pulse. Eight runs were performed in each of these rats.

Optical imaging of intrinsic signals

To target the linear probes and surface electrocorticography (ECoG) arrays to the region of S1 that responded to the electrical stimuli, we first imaged the cortical response using optical imaging of intrinsic signals (Grinvald et al., 1999). Cortical images were obtained using a 15-bit differential data acquisition system (Imager 3001, Optical Imaging Ltd., Rehovot, Israel) with a Pantera 1M60 camera (Teledyne Dalsa, Waterloo, Ontario, Canada) and a 60 mm lens. The camera was mounted above the optical chamber, with its optical axis perpendicular to the cortical surface. We focused the image on the surface of the gray matter and the cortical pial blood vessel in our region of interest (ROI). The ROI we imaged was centered on the atlas coordinates of area S1FL in the left hemisphere (AP 0.00 mm, ML ±4.50 mm, DV –2.5 mm; Paxinos and Watson (2005)), with a matrix of approximately 1000-by-500 pixels, 70-80 pixels/mm, and a 50µm depth of field. The camera frame rate was set to 30 Hz. We imaged the CBV responses to D3, D5 (Figure 1A), and

forepaw stimulation (Figure 1C) under illumination of a green LED light with a center wavelength of 530 nm (isosbestic point).

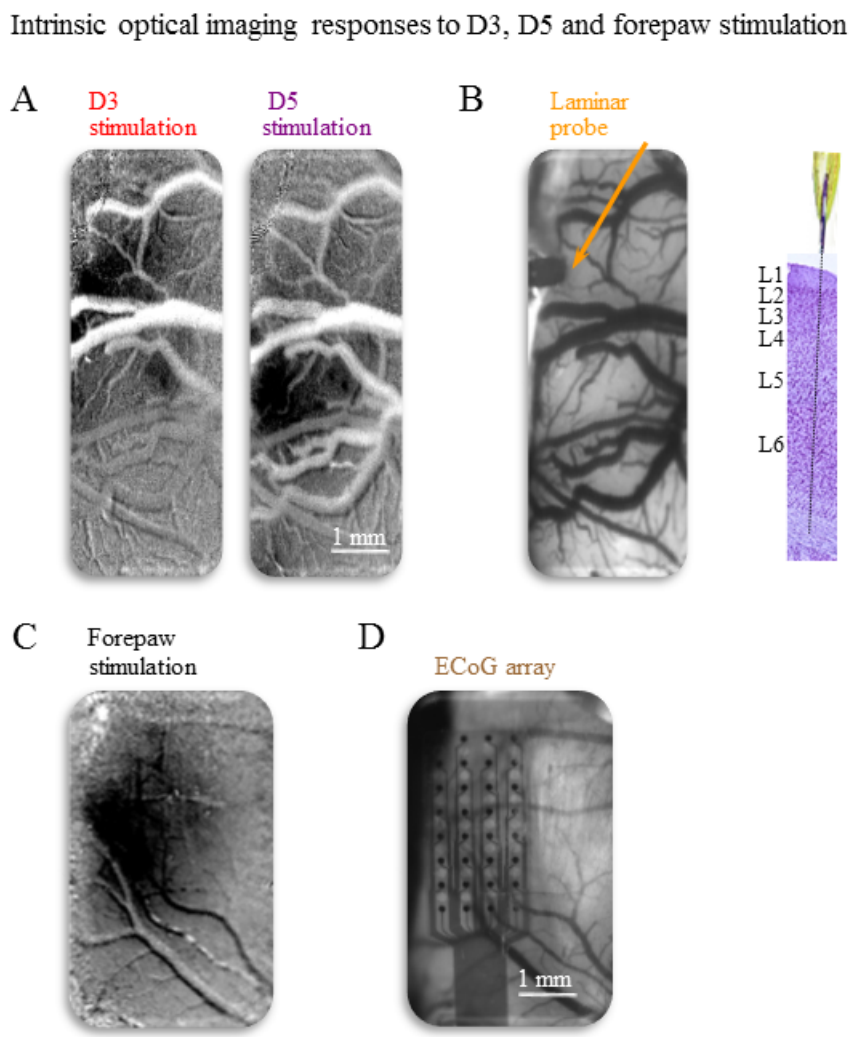

Figure 1. Optical imaging of intrinsic signal responses to D3, D5, and forepaw stimulation. A. The representations of D3 and D5 in area S1FL as identified by the blood volume response to separate stimulations of D3 and D5, imaged optically under the illumination wavelength of 530 nm. Dark regions showed increase in cerebral blood volume. **B.** The image to the left presents the cortical surface and the pial vessels, as imaged under the illumination wavelength of 530 nm. The orange arrow points to the site in which the probe (dark, seen to the left of the arrow) was inserted. A linear probe with 32 microelectrode contacts equally spaced at 100-µm intervals was inserted into the D3 representation of area S1FL. **C.** S1FL representation of the contralateral forepaw, obtained by the blood volume response to electrical stimulation, imaged optically under the illumination wavelength of 530 nm. **D.** An ECoG surface array with 32 contacts, positioned directly on top of the dura above area S1FL of the same brain imaged in C.

Electrophysiology

A linear probe with 32 contacts equally spaced at 100 µm intervals (Neuronexus technologies, Ann Arbor, MI) was inserted into the D3 representation within area S1FL using a manually driven micro-manipulator (David Kopf instruments, Tujunga, CA). All insertions, for both digit and forepaw stimulation studies, were made into the center of the D3 representation, which we estimated based on optical imaging of the CBV response to stimulation of D3. Before each insertion, we verified that the D3 representation we imaged was within area S1FL, as expected based on the rat brain atlas (Paxinos and Watson, 2005).

We monitored the probe insertion angle from multiple points of view, ensuring that the probe was approximately orthogonal to the local cortical surface. To assure coverage of the cortical depth by the contacts, the root mean square (RMS) of signals detected by the bottommost contact was monitored while driving the probe into the cortex. A decrease in RMS indicated when the bottommost recording contact had reached the cortical surface. The probe was then slowly lowered 2.7 mm deeper, spanning the entire thickness of the cortex with approximately four contacts above (within the silicon chamber filled with Hank's Balanced Salt Solution) and approximately five contacts below the cortex (in the white matter) (Figure 1B). Neurophysiological signals were sampled at 24,414.1 Hz using a multi-channel recording system (Tucker Davis Technologies, Alachua, FL).

In separate experiments, we tested whether the epileptic activity was possibly caused by damage to the cortex due to the insertion of the linear probe, which potentially could make the cortex prone to seizures. To this end, surface ECoG recordings were obtained from six rats. The surface ECoG array (NeuroNexus technologies, Ann-Arbor, MI) was centered on the forepaw representation in area S1FL, which was obtained by optical imaging of the CBV response to forepaw stimulation (Figure 1C). The array was placed on top of the dura, leaving the brain intact (Figure 1D). Neurophysiological signals were sampled at 24,414.1 Hz.

Experimental paradigms

Data was obtained from 35 rats under two anaesthetic regimes (dexmedetomidine or urethane). Recordings of responses to either digit or forepaw stimulation were conducted using a linear probe or an ECoG array. Therefore, our data set is comprised of four experimental groups (Table 1):

1. Pilot study; data was acquired from 17 rats using digit stimulation under dexmedetomidine and buprenorphine sedation. Data from each of these rats was recorded with linear probes and included four runs of D3 stimulation, interleaved with four runs of D5 stimulation. The experiments from this group formed two sub-groups of:

a. 67-74 days old rats (n=7),

b. 100-107 days old rats (n=10).

2. Recordings were obtained from six 100-107 days old rats using digit stimulation under urethane anaesthesia. This data was recorded with linear probes and consisted of four runs of D3 stimulation, interleaved with four runs of D5 stimulation.

3. Data from six 100-107 days old rats under dexmedetomidine and buprenorphine sedation was recorded with linear probes while applying forepaw stimulation.

4. Surface ECoG recordings were obtained from six 100-107 days old rats under dexmedetomidine and buprenorphine sedation using forepaw stimulation.

Table 1. Experimental groups.

GROUP	AGE [days]	RECORDINGS	STIMULATION	ANESTHESIA REGIME	# OF ANIMALS
1a	67-74	Linear probe	D3 digit, 4 runs D5 digit, 4 runs	Dexmedetomidine and buprenorphine	7
1b	100-107	Linear probe	D3 digit, 4 runs D5 digit, 4 runs	Dexmedetomidine and buprenorphine	10
2	100-107	Linear probe	D3 digit, 4 runs D5 digit, 4 runs	Urethane	6
3	100-107	Linear probe	Forepaw, 8 runs	Dexmedetomidine and buprenorphine	6
4	100-107	ECoG array	Forepaw, 8 runs	Dexmedetomidine and buprenorphine	6

Preprocessing of electrophysiological data

The mean extracellular field potentials were separated into the high-frequency portion (> 400 Hz), revealing multiunit activity (MUA), and the low-frequency portion (< 400 Hz), revealing the local field potentials (LFP). Action potential detection and sorting based on the high-pass filtered signal were performed offline using 'wave clus' (Quiroga et al., 2004). LFPs were low-pass filtered (cut-off frequency 400 Hz) and resampled at 2000 Hz using a FIR filter with optimal filter order (using Matlab functions: firmpmord.m, filtfilt.m, and resample.m). Noise due to the 60 Hz power-line

frequency, as well as 30 Hz optical imaging interference and harmonic frequencies was removed using an adaptive filtering algorithm based on the Chronux toolbox functions (Bokil et al., 2010). Signal to noise ratio (SNR) was calculated as the ratio between the mean and standard deviation of the evoked signal power over time. The signal from 1 to 2 non-adjacent electrode contacts with low SNR was replaced with a signal interpolated over the neighboring channels using 2D splines (using Matlab function: interp2.m). In practice, we had to replace the data from no more than 2 contacts in each experiment. The current source density (CSD) was calculated using the estimation algorithm based on the second partial derivative of the laminar LFP, ϕ, along the cortical depth z, where Δ is the distance between electrode contacts (Freeman and Nicholson, 1975):

$$\frac{\partial^2 \phi}{\partial z^2} = \frac{\phi(z+2\Delta) - 2\phi(z) + \phi(z-2\Delta)}{4\Delta^2}$$

CSD values from the top and bottom electrode contacts were obtained from Eq. 1, under the assumption of constant field potentials above and below as proposed by Vaknin et al. (1988). An example of depth dependent LFPs and the corresponding CSD response is presented in Figures 2A and B, respectively, with the approximate delineation of cortical layers estimated as described by Sotero et al. (2015).

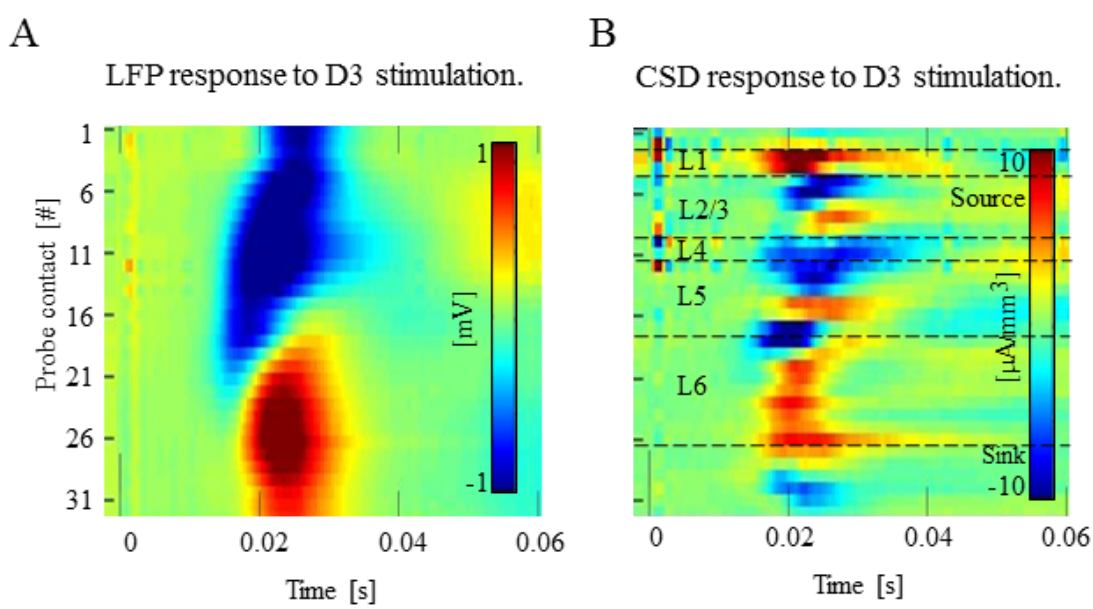

Figure 2. Typical patterns of LFP and CSD responses. A. LFP response to the first pulse (mean over ten trials) of D3 stimulation recorded before seizure induction. **B.** The corresponding CSD response to the first pulse (mean over ten trials) of D3 stimulation, computed using the standard CSD method.

Seizure analysis

The number of epileptic discharges was estimated by visually inspecting the time-courses of the recorded LFP and MUA. In addition to identifying seizures, we also estimated the time of seizure onset and termination relative to the first pulse of the corresponding 10s-long stimulation period. Using the electrophysiological signals, the ictal discharge onset time and duration were estimated for each of the seizures for each animal. Then, for each of the trials, including those with normal evoked activity, seizures, and refractory periods, we estimated the power of HFO ripples (80-200 Hz) and fast ripples (250-600 Hz). We estimated these power measures during three periods of each trial: 5s before the onset of the stimulation period, during the stimulation period, and 5s after the stimulation period.

Statistical evaluation

Values for two or more groups of independent variables were compared using the Student's t-test or one-way ANOVA (IBM SPSS Statistics, 2016). We used the Levene's test to examine whether the variances of the two compared groups were equal. In the cases where equal variances were verified, a Student's t-test or post-hoc Tukey's test was performed to test differences in the means of two or more groups. If there was evidence to support non-equal variances, a post-hoc Tamhane's test or nonparametric Wilcoxon–Mann–Whitney test was applied to evaluate statistical differences between two or more groups. A paired t-test was applied to groups of paired data variables. Results are presented as a mean ± SEM. Differences with $p < 0.05$ were considered statistically significant.

RESULTS

To examine whether peripheral electrical stimulation of the rat's digit or forepaw can induce epileptic activity, we recorded LFP using a linear probe with 32 contacts inserted to the D3 representation in S1FL. The D3 representation was delineated based on optical imaging before inserting the probe and verified against the rat brain atlas.

Pilot study

The susceptibility of the brain to seizure generation is known to depend on age (Migani et al., 2000). Previous studies have shown that the probability of after-discharge occurrence increases with the animal's age (Sperber et al., 1999; Lesser et al., 2008). Aged rats are also more sensitive to excitotoxic neuronal damage and to the epileptogenic effects of kainic acid (Dawson and Wallace, 1992; Sperber et al., 1999; Benkovic et al., 2006; Zhang et al., 2008; Hattiangady et al., 2011). Therefore, in order to optimize our model of epileptic activity and data acquisition, we pursued a pilot study with two age groups of adult rats (Table 1). Our results revealed that seizure induction depended on the animal's age. Seizures were observed in two out of seven 67-74 day old rats, and in six out of ten 100-107 day old animals. Table 2 presents the average number of seizures per rat. The group of older animals (group 1b) presented more epileptic discharges than the group of younger rats (group 1a); however, this trend was not statistically significant. Due to the higher susceptibility of older animals to seizure induction, we performed our subsequent recordings in 100-107 day old animals.

Table 2. Average number of seizures, onset time, and duration of electrographic seizures.

ANIMAL GROUP	MEAN # OF SEIZURES	ONSET TIME [s]	DURATION [s]
1a (67-74 days, digit)	0.42 ± 0.29	0.38 ± 0.07	24.45 ± 2.37
1b (100-107 days, digit)	1.70 ± 0.70	0.56 ± 0.12	30.63 ± 2.56
2 (forepaw, urethane)	–	–	–
3 (forepaw, probe)	18.83 ± 8.49	0.60 ± 0.05	31.50 ± 1.83
4 (forepaw, ECog)	24.16 ± 5.83	0.88 ± 0.09	19.47 ± 1.08

Average number of seizures, onset time relative to the stimulus onset, and duration of electrographic seizures observed in 67-74 and 100-107 day old animals under two different types of anesthetics, stimulations, and recordings. Results are expressed as a mean ± SEM. Statistical tests comparing these measures between groups are mentioned below and in the figure legends.

Characterization of seizures

Figure 3A-C displays the LFP alongside the spectrogram of the ictal discharge induced by somatosensory stimulation of the digit. As seen in Figure 3B, the onset (marked by a red arrow)

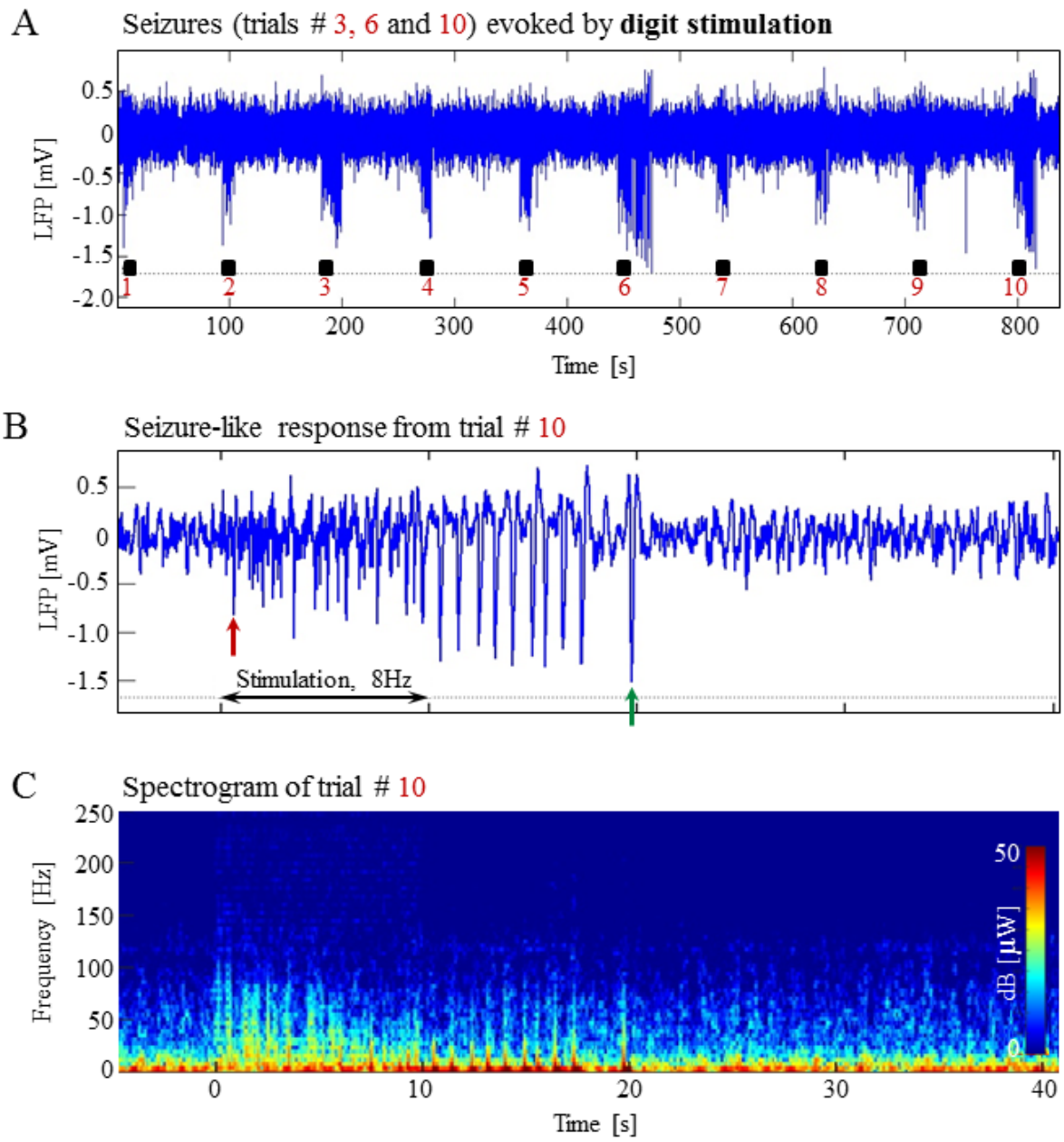

Figure 3. Evoked epileptic activity in response to electrical stimulation of D3. A. LFP recordings of ten trials, each with 10s-long stimulation. The stimulation periods are marked by black rectangles. Each 10s stimulus consisted of a train of electrical pulses delivered at 8 Hz to digit D3. Note that during the third, sixth, and tenth trials, the 10s stimulation evoked an ictal discharge. **B.** The LFP (mean over all contacts spanning the cortical depth) demonstrates a seizure in area S1FL. The red and green arrows indicate the onset and termination, respectively, of an ictal discharge. **C.** A spectrogram (power as a function of frequency and time) computed for the same ictal discharge.

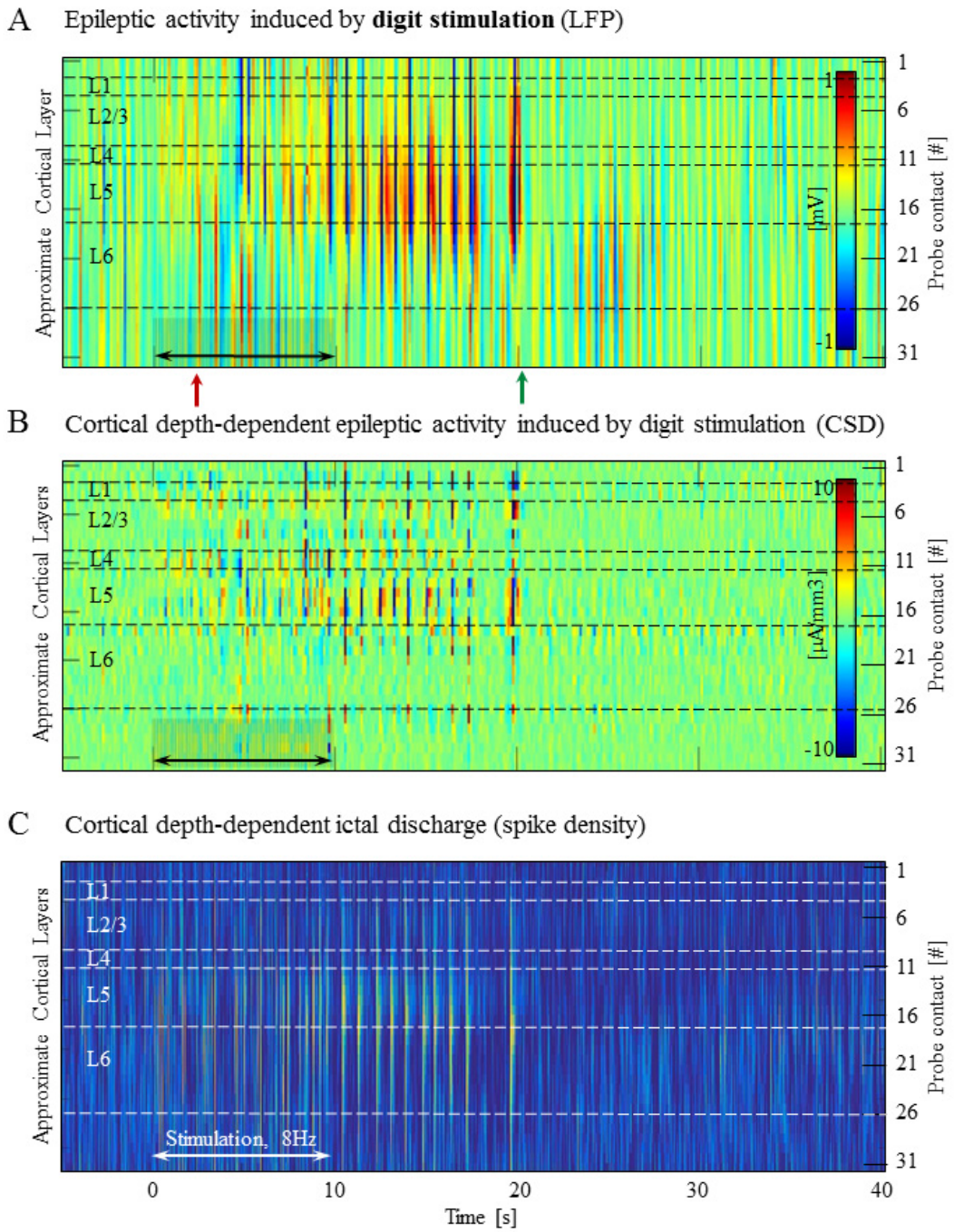

Figure 4. Layer-resolved epileptic activity induced by digit stimulation. A. LFP response to digit D3 stimulation obtained from each of the 32 contacts, showing the spatiotemporal pattern of epileptic activity. **B.** CSD response to digit D3 stimulation demonstrating the same epileptic activity. **C.** The corresponding spike density response shows an ictal discharge. The black (in A, B) and white (in C) horizontal lines represent the approximate delineation of cortical layers, as labeled on the left.

of seizures consisted of high-frequency negative or positive deflections (spikes) of the mean extra-cellular field potential. These events were later replaced by deflections of slower frequency and larger amplitude extending above or below the baseline. These large-amplitude spikes appeared just before the ictal discharge ended (seizure termination is indicated by a green arrow). Figure 4A presents the depth dependent seizure LFP activity, with approximate delineation of cortical layers estimated, as described by Sotero et al. (2015). Figures 4B and 4C present the corresponding CSD and spike density of the ictal discharge, respectively. In most cases, the origin of the ictal discharge was in the deep layers of the cortex, as demonstrated in Figure 4A and B. Repeatable spikes were accompanied by brief and potent sinks followed by slower sources, both visible in the deep cortical layers. A potent slow source in deep layers preceded the termination of the epileptic activity (Figure 4B). The potent sinks and sources in deep layers were associated with increased action potential activity, as illustrated in Figure 4C. Our results are consistent with data obtained from rodent brain slices demonstrating the ability of deep layers to trigger epileptiform events (Yang and Benardo, 2002; Borbely et al., 2006; Adams et al., 2011).

To characterize the differences between normal, seizure-like responses, and the responses during a refractory period, Figure 5A presents a LFP time-course that includes the three types of responses induced by digit stimulation. A typical LFP pattern recorded during a normal evoked response is presented in Figure 5B. The neuronal responses were confined within the 10s period of stimulation. LFP amplitudes arising in response to an electrical pulse were initially higher than the spontaneous LFP amplitudes. Thereafter, the LFP amplitude fluctuated during the 10s stimulation period. Figure 5C presents a time-course typical of the evoked epileptic activity. Seizures were typically characterized by large amplitude spikes in the LFP, poly-spike bursts, and spike-waves throughout the duration of the epileptic activity. Less frequently, rhythmic waves were observed. The ictal discharges typically extended for several seconds beyond the stimulation period and were followed by refractory periods (10 refractory periods out of 17 seizures evoked by digit stimulation). During the refractory periods, a pattern of low-amplitude and slow oscillations was observed (Figure 5D; this time-course is the average of 21 electrode contacts that spanned the cortical depth through all six layers). Less frequently, seizures were followed by a normal response (7 normal responses out of 17 seizures observed with digit stimulation).

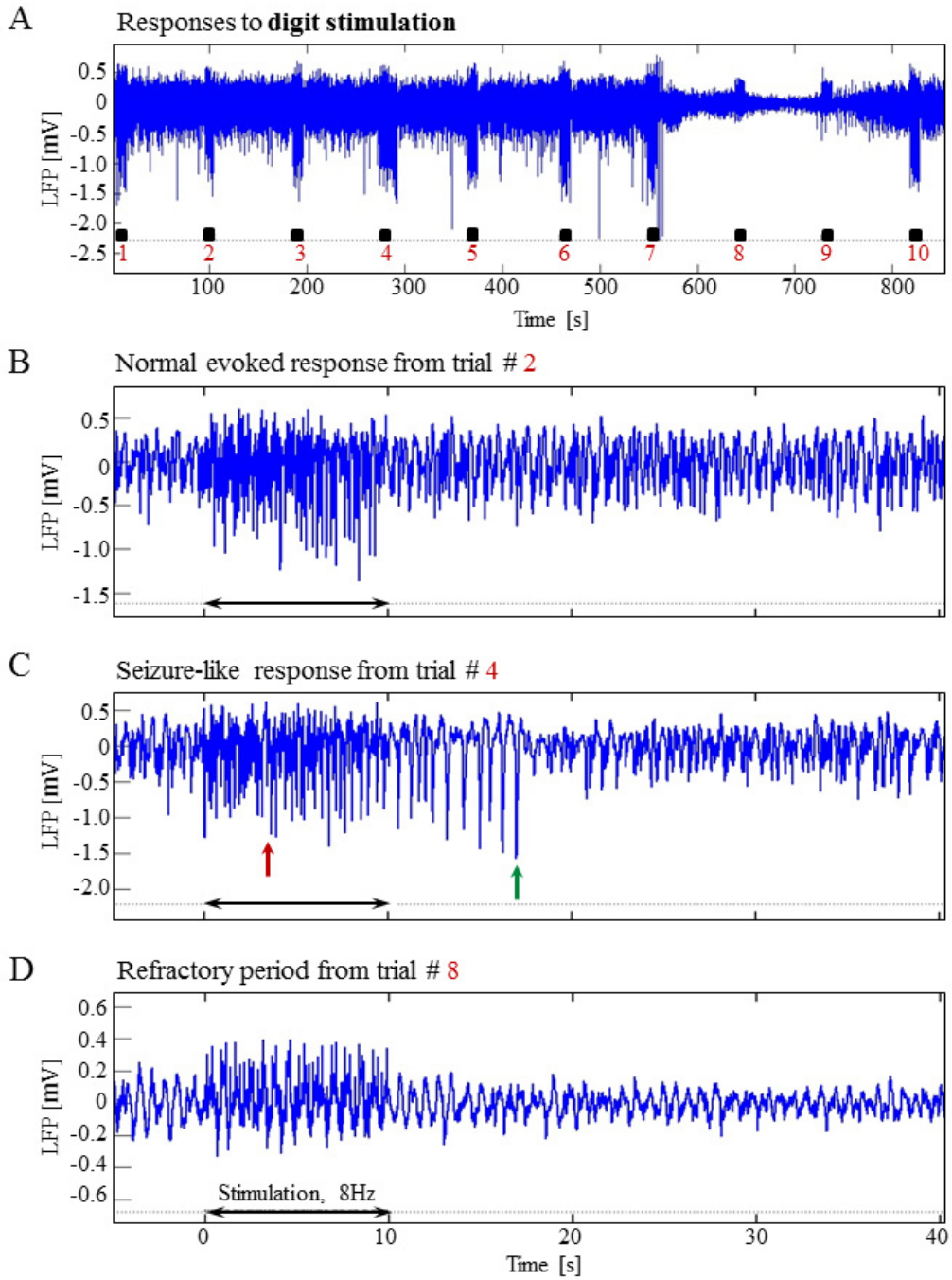

Figure 5. Responses to digit stimulation during normal–, seizure-like–, and refractory periods. A. LFP responses obtained from area S1FL following D3 stimulation. The panel shows ten trials, each with 10s-long stimulation marked by a black rectangle. **B.** Normal evoked responses; the panel shows a magnification of the second trial from A. **C.** A typical activity pattern of an evoked seizure (magnification of the fourth trial from A). **D.** Post-ictal refractory period (magnification of the eighth trial in A). Note that similar LFP patterns were observed in 67-74 and 100-107 day old animals following D3, D5, and forepaw stimulation.

The LFP responses induced by digit or forepaw stimulation were comparable in all animals. Ictal discharges induced by forepaw stimulation were similarly followed by a refractory period (40 refractory periods out of 113 seizures observed with forepaw stimulation) or a normal response (14 normal responses out of 113 seizures). However, in contrast to the events following digit stimulation, ictal discharges induced by forepaw stimulation were followed most frequently by another seizure (55 cases out of 113 seizures). Refractory periods (n=40) were preceded by relatively long epileptic discharges (50.4±2.3s). Normal responses (n=14) were preceded by seizures of shorter duration (27.2±4.1s; $p<0.001$, Tamhane's test for comparing 3 classes, here comparing long and shorter seizures). On average, the first seizure in a pair of sequential seizures was short (17.8±1.2s; n=55; $p<0.001$ between long and short seizures, Tamhane's test).

Seizure susceptibility depends on anesthesia conditions and stimulation types

To determine the factors that influence seizure generation and spread, we applied different methods of anesthesia, recording, and stimulation applied to the D3 digit, the D5 digit, and forepaws.

It is widely accepted that anesthetics modify the balance between excitation and inhibition towards increased relative inhibition, and consequently, they modulate evoked neuronal responses (Franceschini et al., 2010). To evaluate the dependence of seizure generation on the anesthesia regime, six experiments were performed using urethane, an anesthetic that has modest effects on both the inhibitory and excitatory systems and does not affect the noradrenergic system (Hara and Harris, 2002). As illustrated in Figure 6A-C, we did not evoke any seizures with D3 or D5 stimulation in any of the rats under urethane anesthesia.

Neuronal responses in the somatosensory cortex constitute a spatiotemporal interplay between local excitation and surrounding inhibition (Cavanaugh et al., 2002; Derdikman et al., 2003). Derdikman et al. (2003) demonstrated triphasic responses consisting of an early depolarization, a late hyperpolarization, and a subsequent rebound depolarization. The region showing net hyperpolarization is on average more distant from the center of the responding area than the region showing net depolarization. To test whether seizures were more prone to occur right at the representation of the stimulated digit than in a neighbouring region, we alternated stimulations of D3 and D5. With either stimulation of D3 or D5 (or forepaw, below), we recorded

neurophysiological responses in the D3 cortical representation, based on the responses to D3 stimulation measured by optical imaging. On average, a larger number of seizures were detected following D3 stimulation than D5 stimulation; however, this was a non-statistically significant trend (Figure 7; p=0.27, paired t-test).

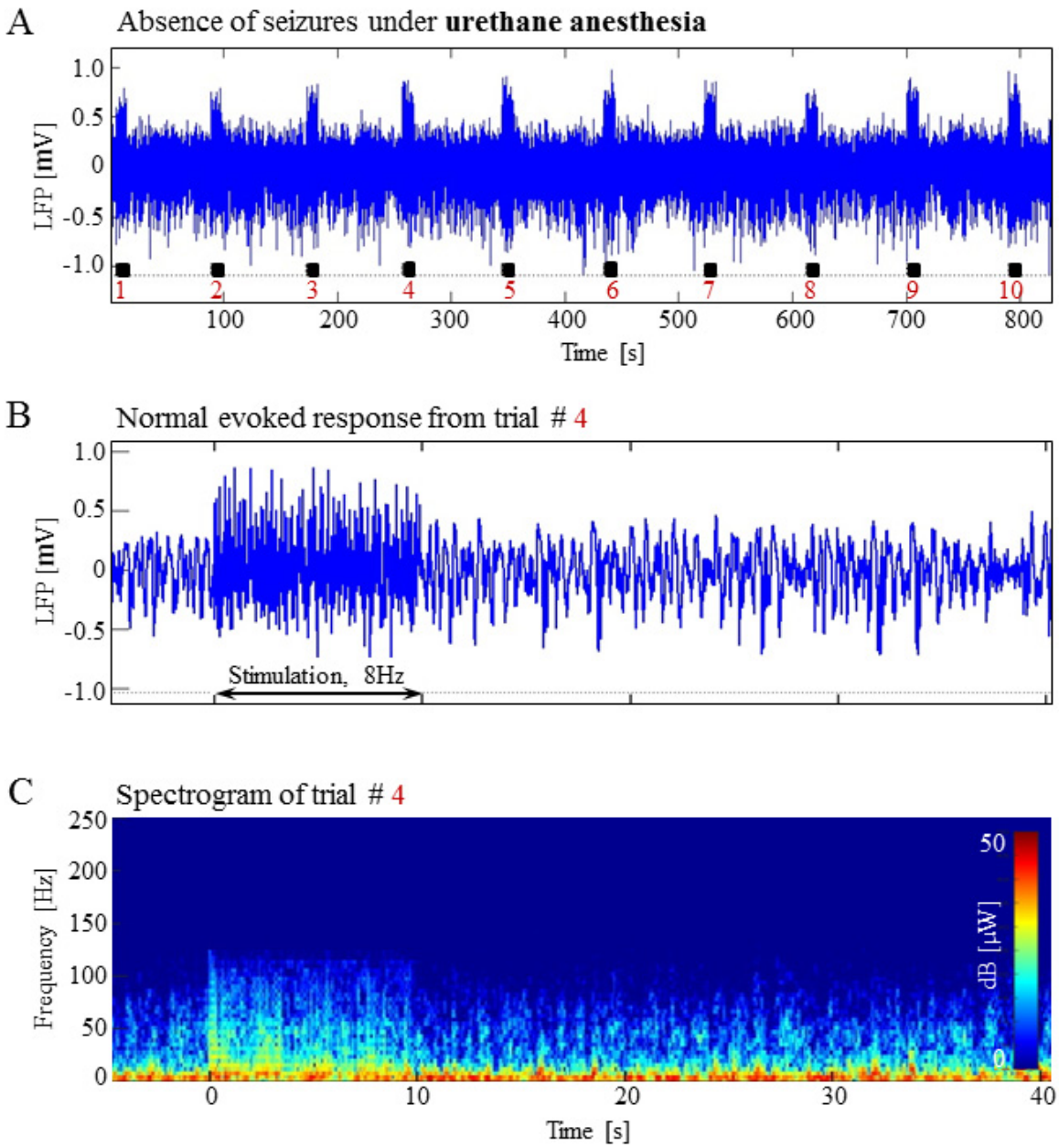

Figure 6. Absence of seizures under urethane anaesthesia. **A.** Ten trials of 10s-long D3 stimulation evoked no seizures following any of the stimulation periods. **B.** Normal LFP evoked responses to digit stimulation from the fourth trial. **C.** Spectrogram computed for the same trial, showing regular responses under urethane anaesthesia.

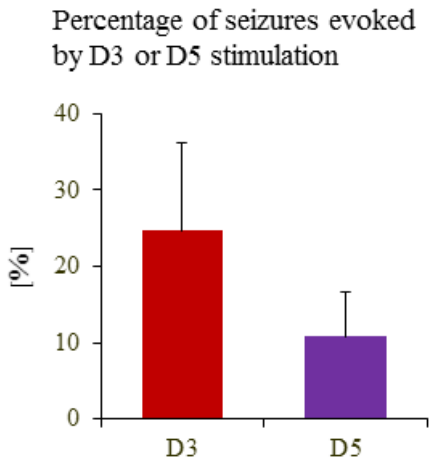

Figure 7. Ictal discharges induced by D3 or D5 stimulation. Percentage of seizures per number of runs of digits D3 (n=45) or D5 (n=35) stimulation. Our recordings in the D3 representation detected a trend of more seizures evoked by D3 stimulation than by D5 stimulation ($p < 0.1$, non-parametric Wilcoxon test).

A balance between local excitation and surround inhibition is required to control the spread of local excitation over long distances (Derdikman et al., 2003). This raised the hypothesis that the seizures we demonstrated with dexmedetomidine and buprenorphine were elicited because our potent stimulation of a digit activated only a small area of cortex (single digit representation) which was insufficient to elicit a comparable surround inhibition. To test this hypothesis, in six rats we applied forepaw stimulation instead of the digit stimulation. The rationale was that forepaw stimulation activates large portions of area S1FL, and therefore it likely elicits more lateral inhibition than single digit stimulation (Waters et al., 1995; Remple et al., 2003). The LFP characteristics of seizures evoked by forepaw stimulation under dexmedetomidine and buprenorphine, including seizure onset and duration, were similar to those evoked by digit stimulation (Figure 8; see details below). However, the percentage of rats that showed seizures during forepaw stimulation (60%) was higher than the corresponding percentage during digit stimulation (28%). In addition, the number of ictal discharges during forepaw stimulation (mean 18.83 ± 8.49 per animal) was higher than the corresponding number of seizures elicited by digit stimulation (1.70 ± 0.70; non-significant trend, $p < 0.1$, nonparametric Wilcoxon–Mann–Whitney test, Table 2).

These results show that seizure vulnerability depends on the anesthesia regime and the type of peripheral stimulation. Sedation with dexmedetomidine and buprenorphine was associated with an increased probability of seizure induction relative to urethane anesthesia. Stimulating a larger cortical region by applying forepaw stimulation induced a larger number of seizures, relative to the number of seizures induced by digit stimulation.

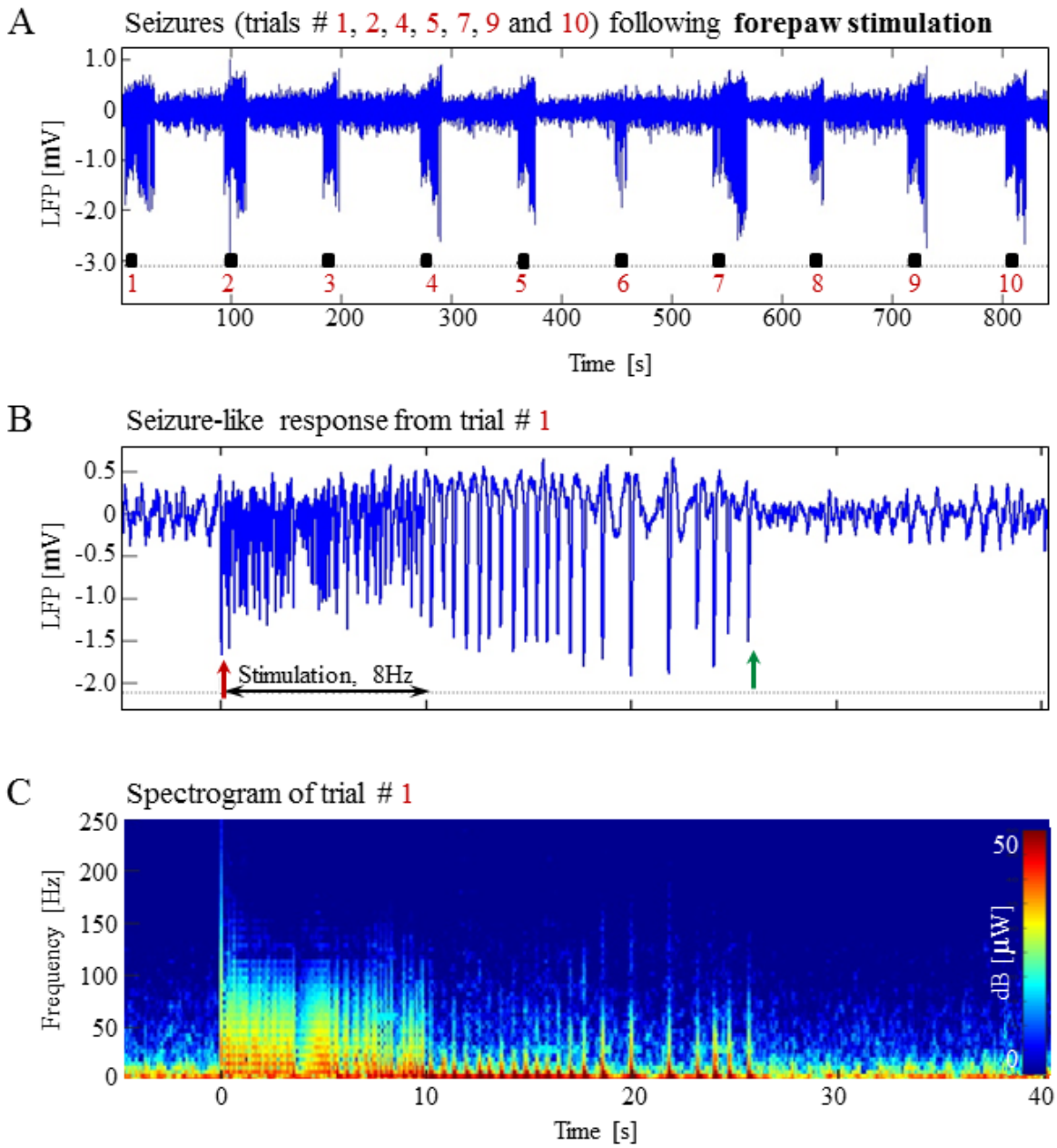

Figure 8. Epileptic activity recorded with a linear probe following forepaw stimulation. A. LFP trace of ten trials, each with 10s-long stimulation. **B.** LFP (mean averaged over 20 electrode contacts spanning the cortical depth) recorded in one trial that showed a seizure pattern. The red and green arrows point to the onset and termination, respectively, of an ictal discharge induced by forepaw stimulation. **C.** Spectrogram computed for the same ictal discharge.

Are the seizures caused by damage to cortex? Seizures recorded with surface ECoG arrays

It is well known that in humans and animals, mechanical damage to cortical brain areas can induce epileptic activity. Specifically, brain injuries can lead to post-traumatic epilepsy (Marks et al.,

1995; Annegers and Coan, 2000; Kharatishvili and Pitkanen, 2010; Curia et al., 2016). To examine whether damage caused by inserting the recording probe into the cortex had an effect on seizure generation, we performed additional experiments using surface ECoG arrays. These arrays were

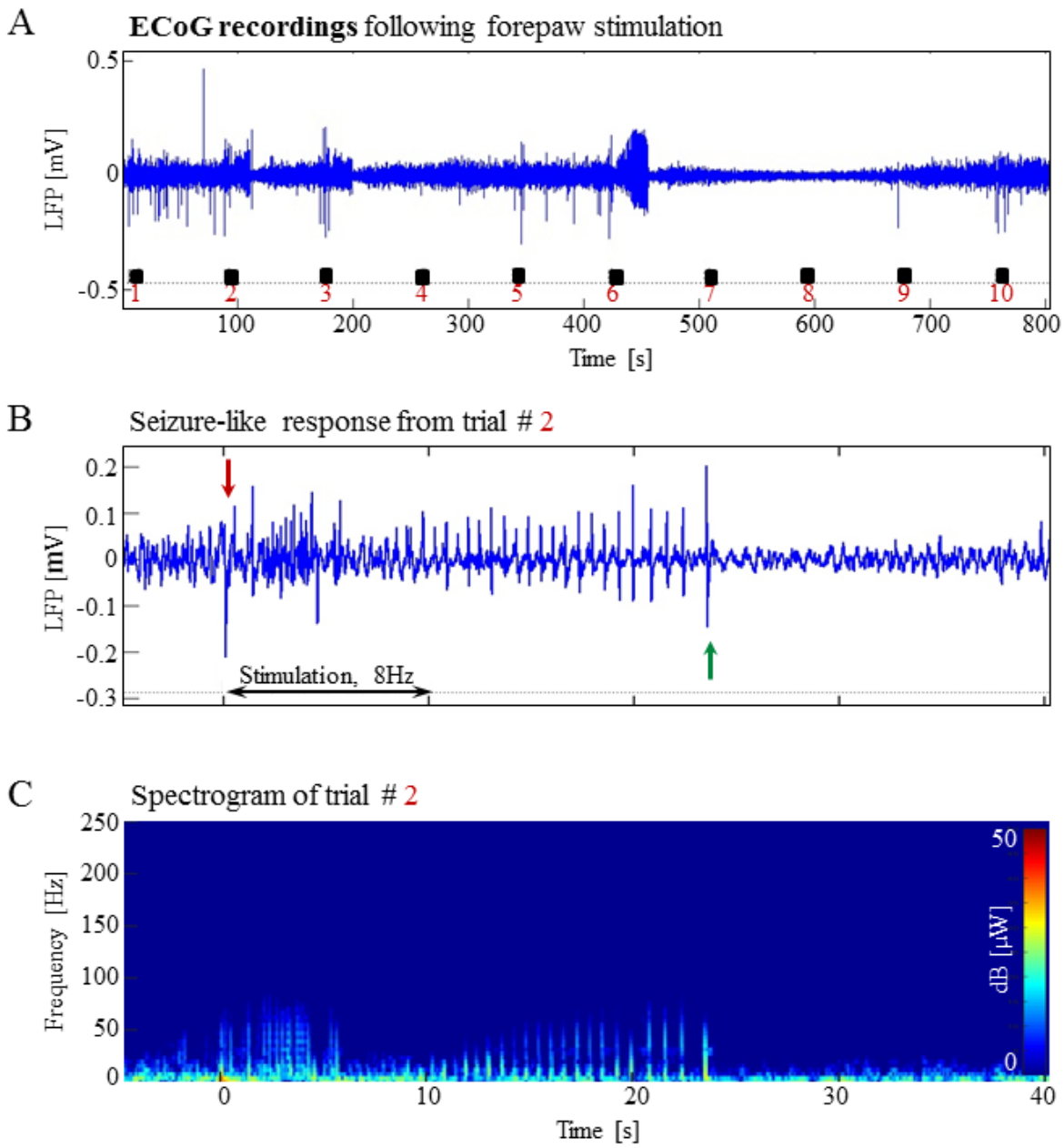

Figure 9. ECoG recordings detect epileptic activity induced by forepaw stimulation. **A.** A time-course averaged over all ECoG contacts: ten trials, each with 10s-long stimulation. **B.** ECoG recordings obtained in the second trial showing seizure activity recorded from the cortical surface. The red and green arrows indicate the onset and termination, respectively, of an ictal discharge. **C.** Spectrogram computed for the same ictal discharge.

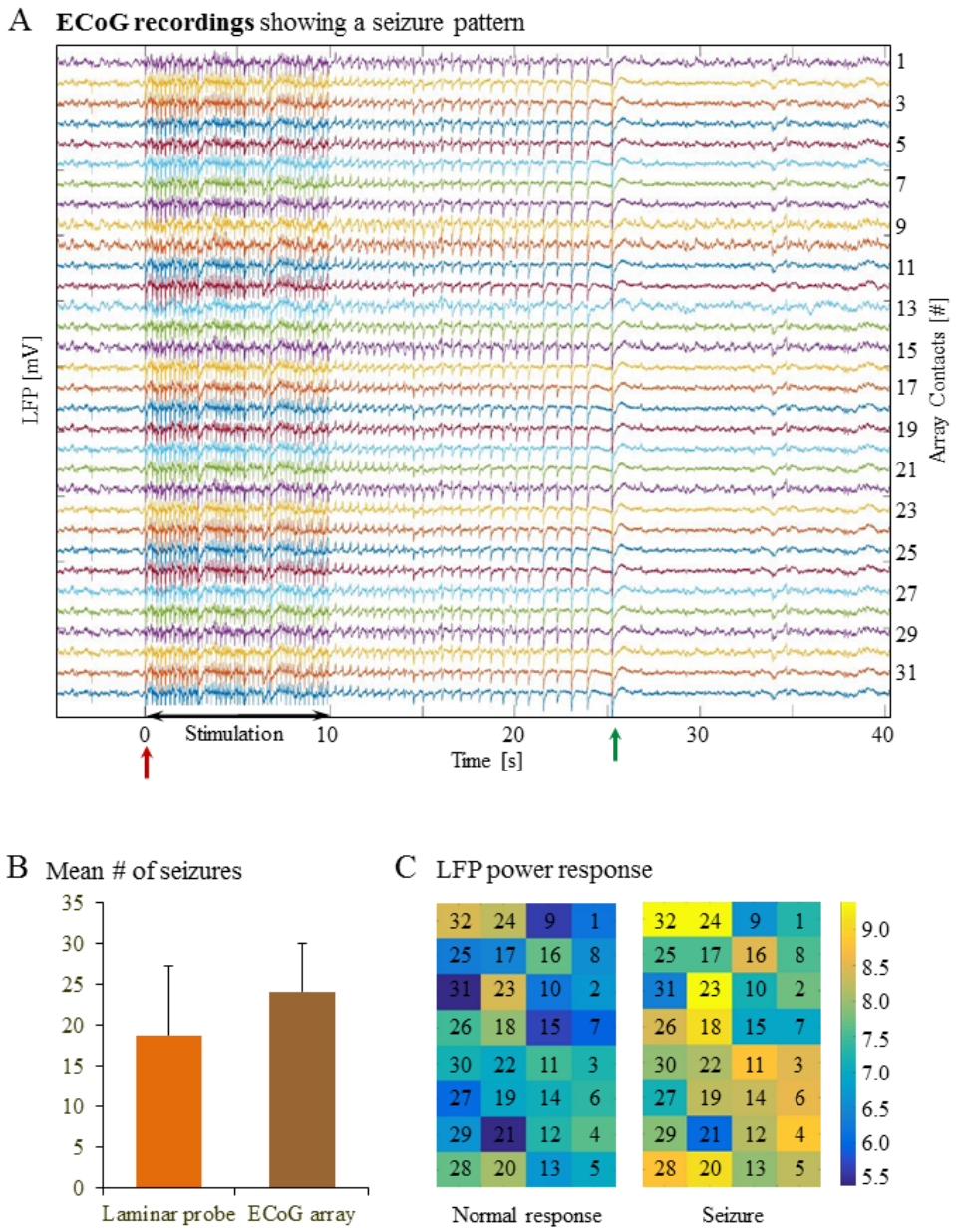

Figure 10. ECoG recordings demonstrating the pattern of an ictal discharge. **A.** ECoG responses obtained from 32 surface contacts during one trial. **B.** Average number of seizures evoked by forepaw stimulation per animal, detected separately by a laminar probe (6 animals, 8 runs per animal, 113 seizures) and a surface ECoG array (6 animals, 8 runs per animal, 145 seizures) are not significantly different (p=0.6, Student's t-test). **C.** Ratio of the power of the broad-band neurophysiological response during stimulation relative to the power during spontaneous activity. The left and right panels present this power ratio without (left) and with (right) seizure, respectively. The ratio is shown in an array form, presenting the power ratio obtained from each of the ECoG contacts in A. The channel numbers make it possible to relate the time-course in A to the pattern of the ECoG array in C.

positioned on top of the dura matter; therefore, they did not cause any damage to cortex. Six rats under dexmedetomidine and buprenorphine sedation underwent forepaw stimulation. In five of six rats (84%) we observed seizures during and following forepaw stimulation (Figure 9A-C, Figure 10A). The number of observed ictal discharges per rat with ECoG recordings was higher than the number observed with intra-cortical probe and forepaw stimulation; however, this trend was not statistically significant (p=0.6, Student's t-test; Table 2, Figure 10B). We concluded that the cortical damage caused by our intra-cortical probes was not a determining factor of seizure generation, since seizure susceptibility to forepaw stimulation was comparable across recordings with linear probes and ECoG arrays.

Do the seizures propagate beyond the somatosensory representation of the forepaw?

Seizures often begin in an acute epileptic focus and spread tangentially to cortex, propagating to other brain regions (Li et al., 2018). For instance, absence seizures originate in neocortex and spread quickly across the brain (Meeren et al., 2002; Li et al., 2018). To estimate the spatial extent of the seizures, we first analyzed the neuronal responses recorded by the ECoG array. The ratio between the LFP power during stimulation and baseline periods was calculated for each ECoG contact in order to visualise the normal response to forepaw stimulation (Figure 10C, left-side panel shows a normal response). We then repeated the same analysis for trials with induced seizures (Figure 10C, right-side panel shows a seizure). ECoG array recordings showed that the normalized power of neuronal activity during a typical seizure was higher than that during the normal response in all contacts of the ECoG array (Figure 10A and C). Therefore, the data recorded by ECoG confirmed that the amplitude of neurophysiological fluctuations is higher during seizures than during normal responses but could not determine differences in the spatial extent of these responses.

To test whether the spatial extent of the seizures is larger than that of the normal responses to digit and forepaw stimulation, we compared the spatial extent of the hemodynamic responses elicited during normal responses to forepaw stimulation to those elicited by seizures. Figures 11A and B present the spatial CBV responses evoked by stimulation of the forepaw, 1s before the stimulus onset (1), 10s after the stimulus onset – which is right at the end of the stimulation period (2), and 20s after the stimulus onset – which is 10s following the cessation of the stimulus (3), for normal evoked response and seizure, respectively. Note that the spatial extent of the active region

immediately following stimulation seems slightly larger when a seizure takes place (Figure 11B, panel 2) than when the response is normal (Figure 11A, panel 2). The spatial extent of the active region 10s following the cessation of the stimulus is clearly larger when a seizure takes place (Figure 11B, panel 3) than when the response is normal (Figure 11A, panel 3). The two time-courses on the right display the corresponding temporal responses from the two brain regions within the activated brain area, which are marked on Figure 11C. At any time-point following the onset of the stimulus, the amplitudes of the CBV responses during the seizure (Figure 11B, red and blue time-courses) were higher than the corresponding amplitudes during normal evoked responses (Figure 11A, corresponding time-courses). The bar plots in Figure 11D present the spatial extent of the responses averaged over six animals, during normal responses and seizures, respectively. For each of the stimulation periods of 5-10s, 10-15s, and 15-20s relative to the onset of the stimulus, the spatial extent of the cerebrovascular hemodynamic changes during seizures (Figure 11B, D) was larger than during normal evoked responses (Figure 11A, D; $p<0.05$ during the stimulation, $p<0.001$ post-stimulation, paired t-test). Note that the two latter periods, namely 10-15s and 15-20s relative to the onset of the stimulus, are part of the post stimulation period in which the ictal discharges persist with no sensory stimulation. Figure 12A, B and D show similar differences between normal and seizure-like responses observed with a digit stimulation ($p<0.05$ during the stimulation, $p<0.001$ post-stimulation, paired t-test). We observed that during seizures the CBV increase extended ~3 mm beyond the normal response, reaching the primary and secondary motor areas (Figures 11B and 12B). Interestingly, not only the average spatial extent of the seizures was larger than that of normal responses obtained during the same period following stimulation, even the spatial extent during seizures *post stimulation* was larger than that observed in normal responses *during stimulation* (Figures 11D and 12D; $p<0.001$, paired t-test). Thus, the seizures we induced propagated beyond the spatial extent of the normal responses to forepaw stimulation.

Figure 11 (see next page). Cerebral blood volume response evoked by forepaw stimulation. A. Cerebral blood volume response evoked by stimulation of the contralateral forepaw. To the left, the spatial responses before (the 1s before stimulus onset), during (9-10s following stimulus onset), and after (19-20s following the stimulus onset) the 10s-long forepaw stimulation period. The reference for obtaining these responses was imaged between 3 and 1 seconds before stimulus onset. Note that negative response indicated in indexed blue color represent increase in absorption of light with wavelength 530 nm, i.e. increase in blood volume. To the right are two time-courses presenting the corresponding temporal response from two regions (blue and red ROIs in C) within

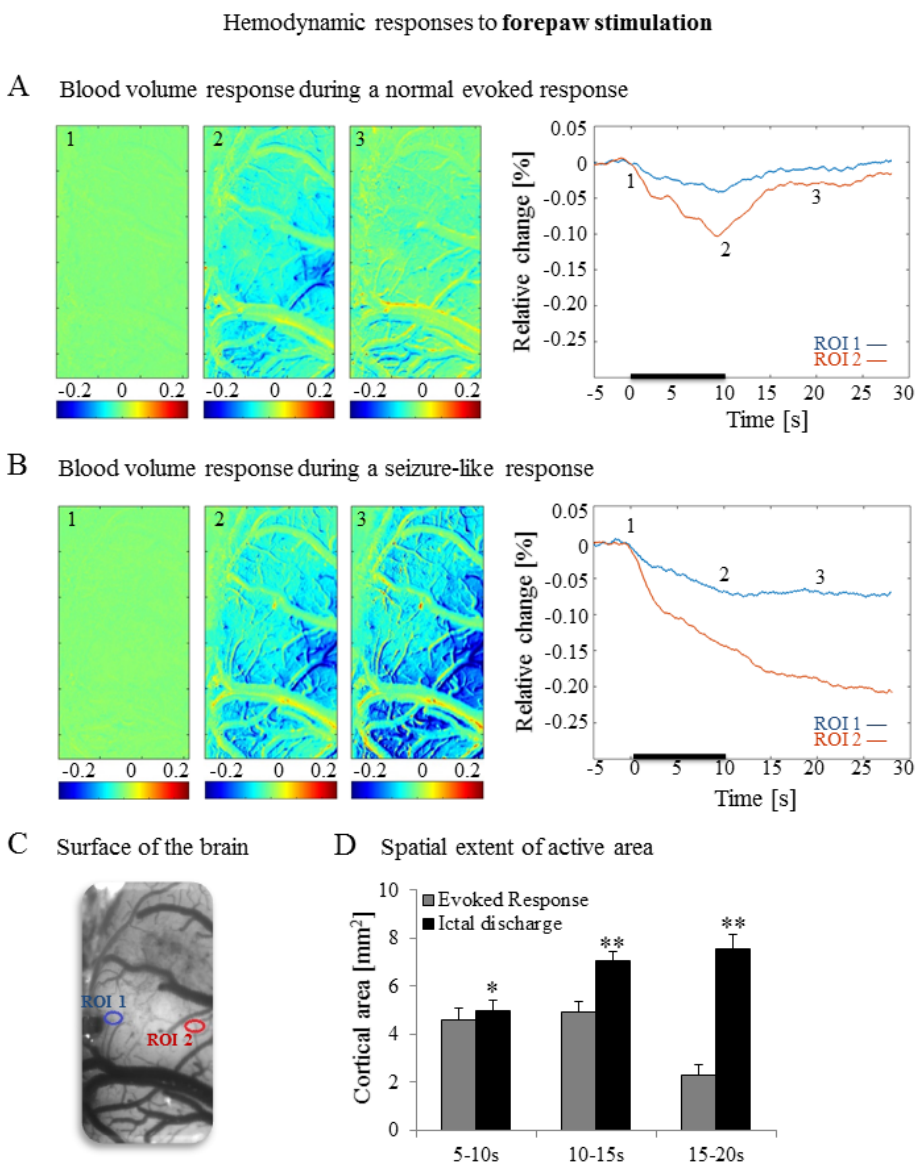

Figure 11 (continued). the activated area. The stimulation period between 0 and 10 seconds is marked by a dark bar. **B.** Maps of the blood volume changes during seizure-like response from before, during, and after the 10s-long forepaw stimulation period (exact time periods are as in A). To the right are two time-courses presenting the corresponding temporal response from two regions (blue and red ROIs in C) within the activated area. **C.** The imaged cortical surface with the two ROIs used for sampling the time-courses presented in A and B. **D.** A bar graph showing the spatial extent of the activated cortical region calculated for the epochs of 5-10s, 10-15s, and 15-20s relative to the onset of the stimulus during normal evoked (n=21) and seizure responses (n=21; * $p<0.05$, ** $p<0.001$; paired t-test between normal evoked response and ictal discharge). We calculated the spatial extent of the response trial by trial by applying a threshold (here, 3%) to the blood volume response in space. The same threshold was applied to all 3 periods of the normal evoked response and seizure.

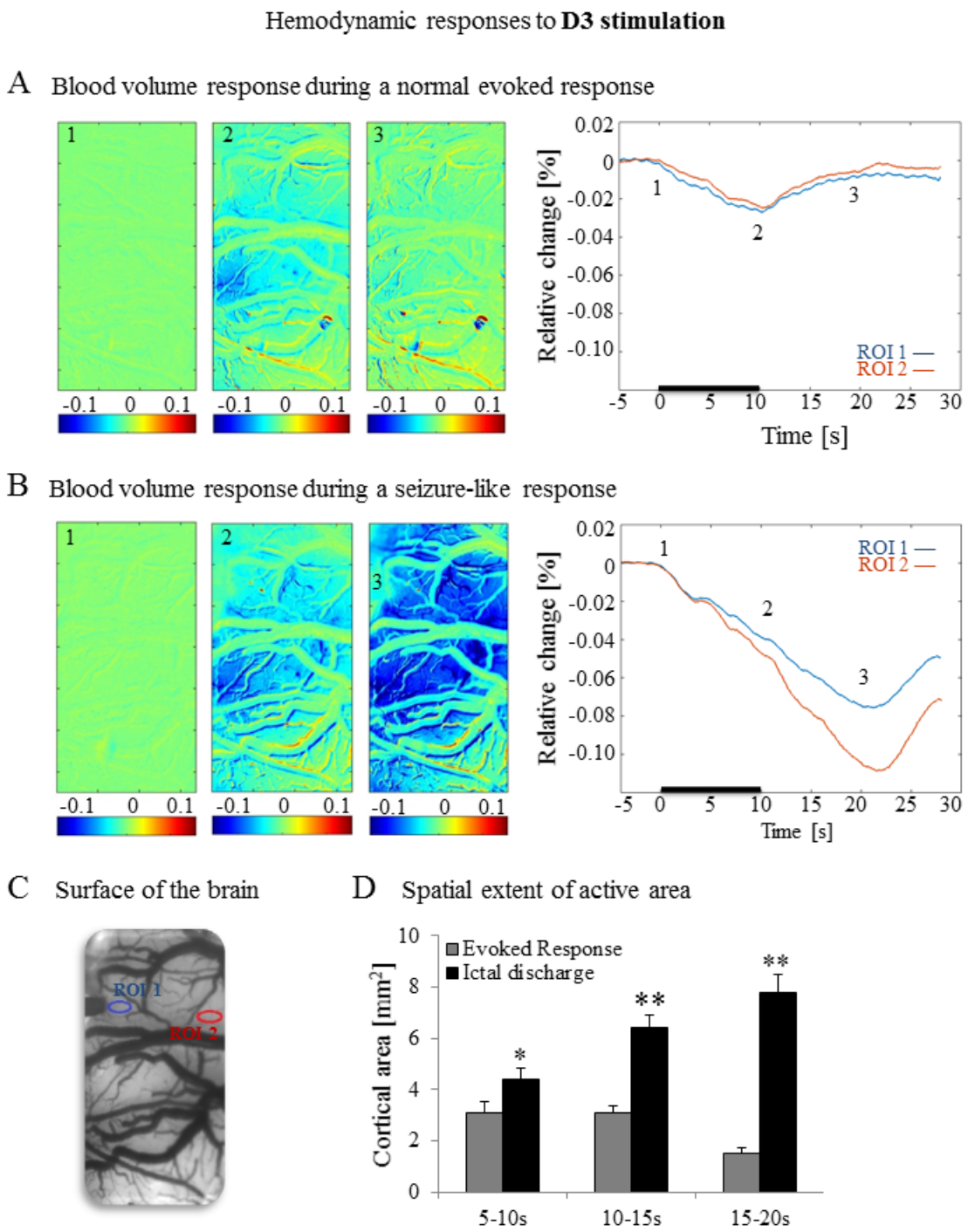

Figure 12. Cerebral blood volume response evoked by D3 stimulation. A. The format of presentation is identical to that used for Figure 11. In **D**, we calculated the spatial extent of the response trial by trial by applying a threshold (here, 2%) to the blood volume response in space. The same threshold was applied to all 3 periods of the normal evoked response and seizure.

Latency of the seizure onset and seizure duration

The characteristics of epileptic activity were evaluated for each group of rats. First, the seizure onset time and termination were marked by visual inspection (Figure 3, Figure 4). By examining the LFP amplitudes and the corresponding spectrograms, the seizure onset time was calculated relative to the first stimulation pulse. Analysis of the seizure onset time revealed no significant differences between the rats of the two age groups (Table 2). In addition, there were no statistical differences in seizure onset time between digit and forepaw stimulations and between recordings made with linear probe and ECoG array recordings (Figure 13A).

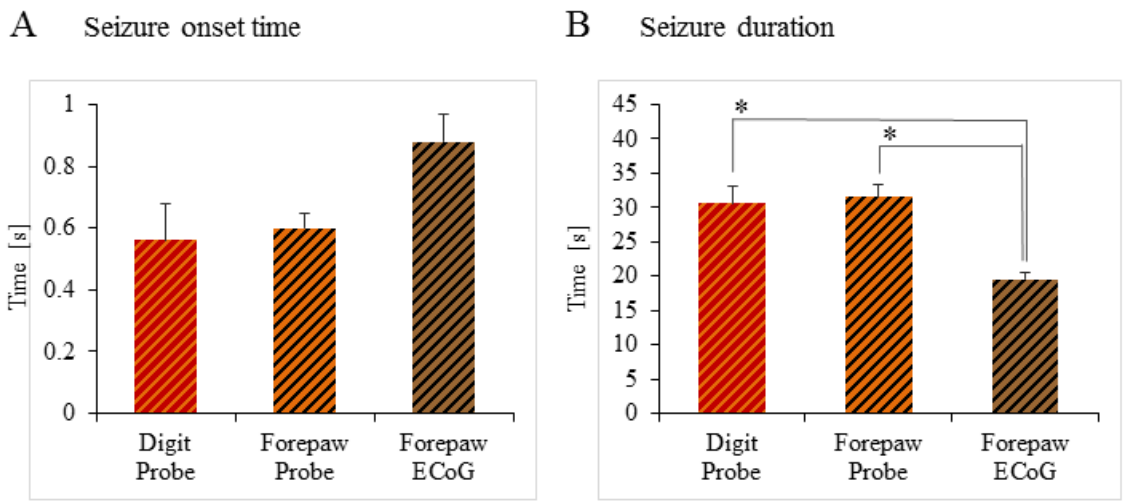

Figure 13. Means of onset times and durations of ictal discharges induced under different conditions: digit/forepaw stimulation and intra-cortical/surface recordings. A. A bar graph presenting seizure onset time relative to the onset of the stimulus estimated in animals that went through digit stimulation and recordings with laminar probes (n=17 seizures) and forepaw stimulation and recordings with either laminar probes (n=113 seizures) or ECoG arrays (n=145 seizures). **B.** A bar graph showing the duration of seizures evoked by stimulating digits (laminar probe, n=17 seizures) or the forepaw (laminar probe, n=113 seizures; ECoG array, n=145 seizures). The bars present mean ± SEM. Note the statistically significant differences in seizure duration between probe and ECoG recordings (* $p<0.05$; Tamhane's test).

Previous studies in humans and animal models reported seizure durations in the range of a few seconds to more than five minutes. A seizure lasting longer than five minutes is considered as status epilepticus (Grover et al., 2016). All seizures evoked in our rats were brief, lasting less than one minute. Using linear probe recordings, the durations of seizures evoked by digit or forepaw

stimulations were comparable. However, the average duration of seizures recorded with the ECoG array was shorter than that obtained with linear probe recordings ($p<0.05$; Tamhane's test; Table 2, Figure 13B).

High-frequency oscillations

In the rat neocortex, somatosensory-evoked HFOs can be identified in the normal LFP response. Similarly, HFOs can be observed in seizure-associated pathological activity in the visual and sensorimotor cortex of animals (Murthy and Fetz, 1996; Jefferys et al., 2012). We therefore investigated whether HFOs coincided with the ictal discharges in our animal model. Under dexmedetomidine and buprenorphine sedation, we observed ripples and fast ripples that preceded and coincided with all episodes of ictal discharges induced by peripheral somatosensory stimulation (Figure 14A-B). The power of fast ripples during the 5s prior to stimulation associated with ictal discharges was higher relative to the power observed prior to normal responses and refractory periods ($p<0.05$; Tamhane's test; Figure 14D; Table 3). The power of fast ripples following the end of stimulations associated with ictal discharges was higher than the corresponding power associated with normal evoked responses and refractory periods ($p<0.001$; Tamhane's test; Figure 14D; Table 3).

With forepaw stimulation, the power of ripples during seizures was higher than the corresponding power during refractory periods before and after the stimulation period ($p<0.001$; Tamhane's test; Figure 15A, Table 3). The power of ripples following seizures was higher than the power observed following normal evoked responses after the stimulation period ($p<0.001$; Tamhane's test; Figure 15A, Table 3). The power of fast ripples before seizures was higher than the power observed before responses during the refractory period ($p<0.001$; Tamhane's test; Figure 15B, Table 3). The power of fast ripples during the stimulation periods associated with evoked responses and ictal discharges was higher than the power observed during stimulation during the refractory period ($p<0.001$; Tamhane's test; Figure 15B, Table 3). The power of fast ripples following seizures was higher than the power observed following normal evoked responses and following responses during refractory periods ($p<0.001$; Tamhane's test; Figure 15B, Table 3).

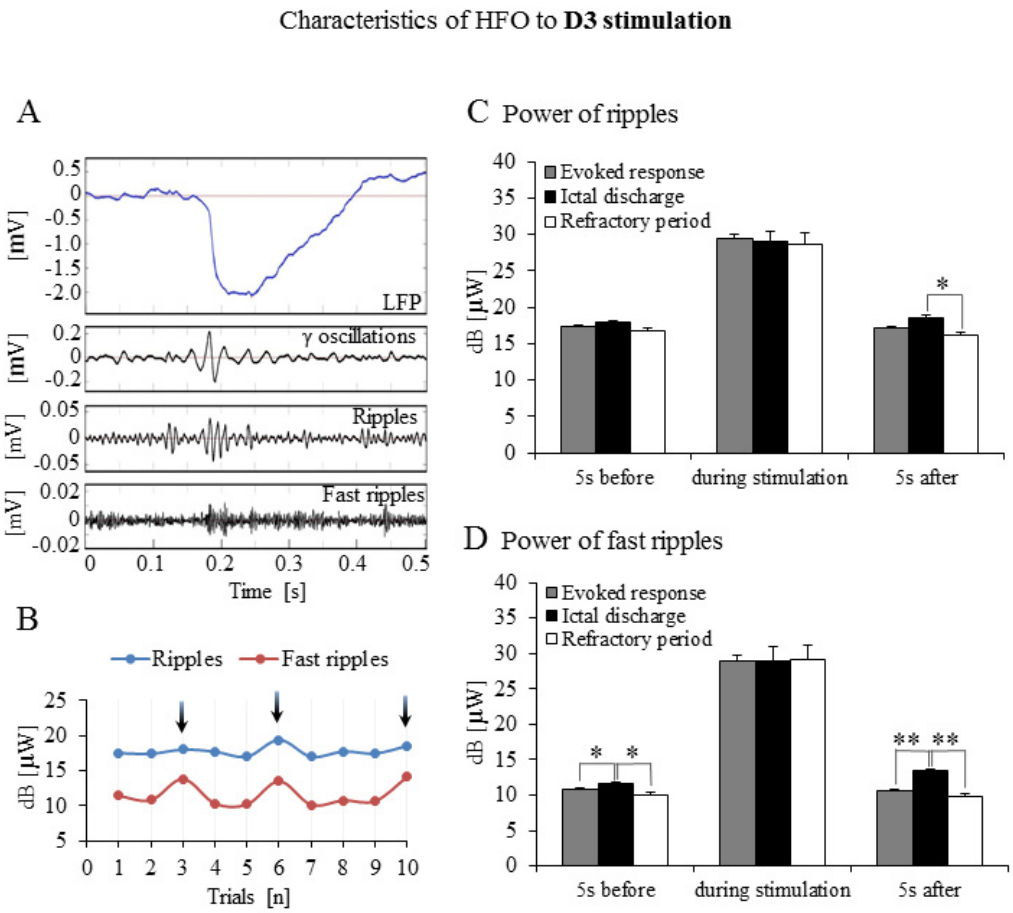

Figure 14. HFOs in response to D3 peripheral somatosensory stimulation. A. LFP recorded from area S1FL showing a seizure spike with simultaneously occurring ripples (80-200 Hz) and fast ripples (250-600 Hz) following stimulation of D3. High frequency oscillations coincided with all episodes of ictal discharge induced by digit or forepaw stimulation. **B.** A representative example of the power of ripples and fast ripples corresponding to the 5s period after the cessation of stimulation. The black arrows indicate the trials with seizures. Similar variations in the power of HFOs were observed in all animals following digit or forepaw stimulation. **C.** A bar graph showing the average power of the ripples 5s before, during, and 5s after the stimulations associated with normal evoked response (n=129 trials), ictal discharge (n=21 trials), and refractory period (n=20 trials). Results are shown as a mean ± SEM. Note the statistically significant difference between Ictal Discharge and Refractory Period (* $p<0.05$; Tamhane's test) following the offset of the stimulation. **D.** Average power of the fast ripples 5s before, during, and 5s after the stimulation associated with normal evoked response (n=129 trials), ictal discharge (n=21 trials), and refractory period (n=20 trials). Statistically significant differences were observed between normal Evoked Response and Ictal Discharge before and after the stimulation period, and between Ictal Discharge and Refractory Period before and after the stimulation period (* $p<0.05$, ** $p<0.001$; Tamhane's test).

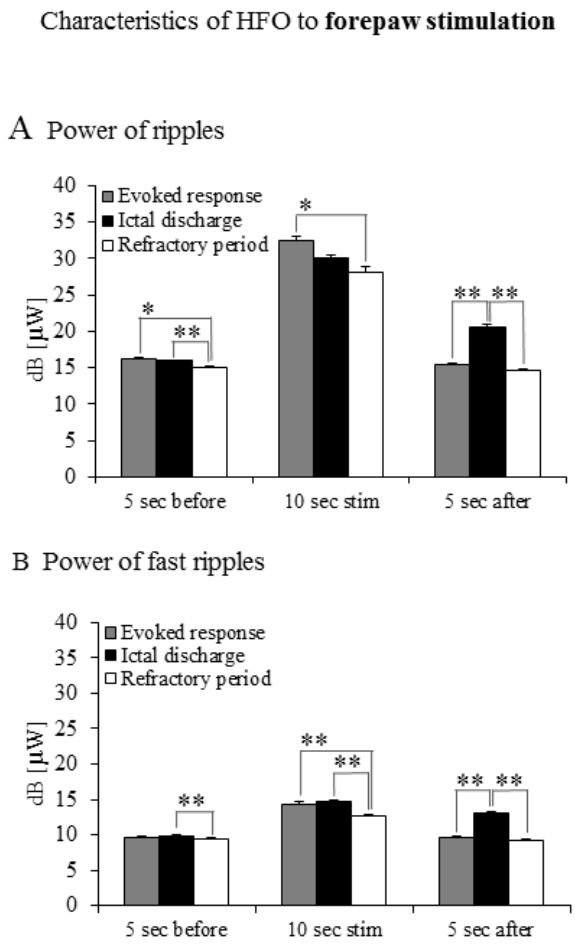

Figure 15. HFOs in response to forepaw stimulation. A. A bar graph showing the average power of the ripples 5s before, during, and 5s after the stimulations associated with normal evoked response (n=50 trials), ictal discharge (n=110 trials), and refractory period (n=50 trials). Results are shown as a mean ± SEM. Note the statistically significant differences between Evoked Response and Refractory Period, Evoked Response and Ictal Discharge, and Ictal Discharge and Refractory Period (* $p<0.05$; ** $p<0.001$; Tamhane's test). **B.** Average power of the fast ripples 5s before, during, and 5s after the stimulation associated with normal evoked response (n=50 trials), ictal discharge (n=110 trials), and refractory period (n=50 trials). Statistically significant differences were observed between Evoked Response and Refractory Period, Evoked Response and Ictal Discharge, and Ictal Discharge and Refractory Period (** $p<0.001$; Tamhane's test).

Lastly, for normal evoked responses, ictal discharges, and refractory periods, the power of ripples and fast ripples during stimulation was higher than the power observed during the 5s periods before and after the stimulation with digits ($p<0.001$; Tamhane's test; Figure 14C-D, bars in the middle; Table 3) and forepaw ($p<0.001$; Tamhane's test; Figure 15A-B, Table 3).

Table 3. Power of the ripples and fast ripples.

		RIPPLES dB[μW]			FAST RIPPLES dB[μW]		
		Before stimulation	Stimulation period	After stimulation	Before Stimulation	Stimulation period	After stimulation
DIGITS	Evoked response	17.4±0.16	29.5±0.61	17.1±0.17	10.9±0.18	28.9±0.870	10.6±0.17
	Ictal discharge	18.0±0.17	29.1±1.42	18.5±0.50	11.7±0.16	29.0±1.87	13.5±0.20
	Refractory period	16.7±0.41	28.7±1.62	16.2±0.38	10.0±0.38	29.2±2.00	9.8±0.41
FOREPAW	Evoked response	16.2±0.21	32.4±0.72	15.5±0.17	9.7±0.07	14.4±0.23	9.6±0.13
	Ictal discharge	16.0±0.11	30.1±0.29	20.6±0.43	9.9±0.04	14.8±0.18	13.0±0.19
	Refractory period	15.1±0.15	28.2±0.69	14.7±0.14	9.5±0.07	12.6±0.25	9.3±0.10

The power (mean ± SEM) of the ripples and fast ripples during normal evoked responses, ictal discharges, and refractory periods observed in animals following digit (n = 20 seizures) and forepaw (n = 113 seizures) stimulations. The power of the ripples and fast ripples was calculated for the periods 5s before, 10s during, and 5s after the stimulation.

DISCUSSION

Based on the experiments presented here, we have described five main findings. First, electrical stimulation administered peripherally to the rat digits D3 or D5, as well as to the forepaw, produces electrographic seizures. Second, seizure susceptibility depends on anesthesia conditions: sedation with dexmedetomidine increases the probability of seizure induction in comparison to anesthesia with urethane. Third, seizure susceptibility also depends on the spatial extent of the stimulated region, i.e. single digit or forepaw representation. Fourth, the evoked seizures propagate to adjacent brain cortical regions, beyond the spatial representation of the stimulated digit or forepaw. Fifth, high-frequency oscillations precede and coincide with all epileptic discharges evoked by peripheral stimulation.

Importantly, the ictal discharges we induced by peripheral electrical stimulation form a new animal model of somatosensory-evoked reflex seizures. This model is free of electrical artifacts and does not involve damage to the brain caused by insertion of a stimulating electrode or application of chemo-convulsant.

Characteristics of induced reflex seizures

Our findings indicate that electrical somatosensory stimulation of naïve rat digits or forepaw forms an animal model of reflex seizures. Reflex seizures are defined as seizures triggered by sensory stimulation, which is usually patient-specific (Guerrini et al., 1992; Striano et al., 1992; Panayiotopoulos, 2005; Striano et al., 2012; Sala-Padro et al., 2015; Wolf, 2015). In epileptic patients, TIS can be evoked by a cutaneous-mucosal sensorial stimulus and is limited to specific skin regions (Striano et al., 2012; Sala-Padro et al., 2015). Focal areas that are sensitive to these stimuli include the foot, finger, arm, shoulder, chest, face, and head (Deonna, 1998). In humans, somatosensory-evoked seizures can be also induced by the electrical stimulation of peripheral nerves (Deonna, 1998). In majority of patients affected by TIS, the sensory stimulations that induce seizures are repetitive and last 5-20 seconds (Kanemoto et al., 2001; Hsieh et al., 2011; Sala-Padro et al., 2015). To trigger the epileptic activity in our animals, we followed a similar approach to somatosensory stimulation. The electrical stimuli we delivered to the digit or forepaw were repetitive and lasted 10 seconds. Another feature of our seizure model similar to TIS in humans is that TIS are brief and frequently followed by a refractory period (Deonna, 1998; Hsieh et al., 2011; Striano et al., 2012; Sala-Padro et al., 2015). All of our animals displayed similar, brief electrographic seizures that were followed by a refractory period, normal response, or another seizure. Refractory periods were preceded by relatively long epileptic discharges. Normal responses were preceded by seizures of shorter duration. The first seizure in a pair of sequential seizures was short on average. Long seizures involve sustained neuronal excitation and the use of neurotransmitters such as glutamate. This may require a recovery time for the excitable membrane to be ready for a second stimulus (Dorn and Witte, 1995; Revilla et al., 1999).

The repetitive nature of stimulation we applied is reminiscent of kindling procedures. Kindling is commonly induced by application of repetitive, focal, sub-convulsive electrical stimulations *directly* to specific brain structures (such as the amygdala or hippocampus), leading to after-discharges and electrographic seizures (Goddard et al., 1969; Morimoto et al., 1987; Barnes and

Pinel, 2001; Gorter et al., 2016; Loscher, 2017b). After-discharges can be triggered by electrical stimulation administered directly to different brain regions, including cortical area S1 (Racine, 1975; Lesser et al., 2008; Kalamangalam et al., 2014). They are temporally similar to spontaneous epileptic activity (Lesser et al., 1999; Blume et al., 2004). Importantly, kindling is induced by direct stimulation of the brain's tissue, whereas the seizures we present here are induced by peripheral sensory stimulation.

The neocortex is one of the brain structures involved in several types of acquired epilepsy, including TIS (Timofeev et al., 2014; Chauvette et al., 2016). Cortical seizures are characterized by spike– and polyspike–wave electrographic discharges at 1.0–2.5 Hz, as well as fast oscillations (Boucetta et al., 2008; Timofeev et al., 2014) that are followed by the formation of larger amplitude spike– and polyspike–wave field potential complexes (Timofeev and Steriade, 2004). A similar pattern of epileptiform electrographic activity is observed in our animal model of reflex seizures (e.g., Figure 3B).

In an epileptic brain, cortical seizures elicit a focal, large-amplitude increase in utilization of glucose and oxygen, cerebral blood vessel dilatation, and an increase in blood flow and volume (Engel et al., 1982; Lauritzen and Gold, 2003; Patel et al., 2013). Traditional models of seizure propagation involve the assumption of an onset zone and a progressive outward spread of activation (Ma et al., 2013). Neuroimaging techniques, such as intrinsic optical imaging, indirectly measure neuronal activity based on changes in CBV and oxygenation. Intrinsic optical imaging under illumination of an isosbestic wavelength such as 530 nm is directly proportional to increases and decreases in CBV (Zhao et al., 2009; Ma et al., 2013). As shown in previous studies, intrinsic optical signal can be used to identify ictal initiation and early propagation (Bahar et al., 2006; Zhao et al., 2009). In our animal model, all epileptic events induced by digit or forepaw stimulation affected the CBV. All seizures began focally and propagated horizontally through the cortex. The entire S1FL region and parts of surrounding cortical areas displayed a steady increase in CBV (Figures 11B and 12B). The spatial extent of the CBV response to the ictal discharges was larger than the S1FL representation of the stimulated digit or forepaw. In addition, the spatial extent of the CBV response to seizures increased with time, confirming that ictal discharges are prone to cortical spread. The epileptic responses we elicited show characteristics similar to those demonstrated by Haglund and Hochman (2007) using optical imaging of intrinsic signals, where seizures were induced by focal application of bicuculine to the cortical surface. In addition, similar

hemodynamic responses were observed during seizures evoked by focal administration of penicillin directly onto cortex (Chen et al., 2000), bicuculine (Suh et al., 2005) and 4-aminopyridine (Schwartz and Bonhoeffer, 2001; Ma et al., 2013; Harris et al., 2014). Harris et al. (2018) specified that during focal seizures induced in deep cortical layers the neurovascular coupling is preserved but is associated with periods of tissue hypoxia. Lastly, in humans affected by neocortical epilepsy, epileptiform events increase CBV and the signal spreads widely throughout the cortex, mirroring our animal seizure data (Shariff et al., 2006).

Characteristics of the anaesthetic regime and stimulation type

In the present study, ictal discharges were evoked under dexmedetomidine sedation. This type of sedation possesses neuroprotective characteristics such as optimized cerebral oxygen supply and decreased intracranial pressure and CBV during surgery (Bekker and Sturaitis, 2005; Gerlach and Dasta, 2007). It has been reported that under continuous intravascular systemic perfusion of dexmedetomidine for more than two hours, forelimb stimulation elicits seizure-like responses observed in LFP, accompanied by changes in cerebral blood flow (Fukuda et al., 2013). Indeed, it was suggested that the use of dexmedetomidine *per se* modulates central adrenergic function by activating presynaptic α_2-adrenergic receptors, which in turn increases sensitivity to seizure expression (Oishi and Suenaga, 1982; Gertler et al., 2001). In contrast, Whittington et al. (2002) demonstrated that dexmedetomidine suppresses the induction, generalization, and severity of seizures induced by intravenous administration of cocaine. Moreover, it was reported that medetomidine sedation does not increase seizure vulnerability, nor does it affect LFP and BOLD responses during epileptic activity (Airaksinen et al., 2010; Airaksinen et al., 2012). Seizure activity (frequency and onset time) evoked by kainic acid was similar in the awake and medetomidine-sedated rats (Airaksinen et al., 2010; Airaksinen et al., 2012). Consistent with the findings by Whittington et al. (2002) and Airaksinen et al. (2012), we did not evoke any seizures with short forelimb stimuli protocols (1s stimulation of 8 Hz with 0.6-0.8 mA) under the same anesthetic condition (Sotero et al., 2015). Therefore, based on data of Whittington et al. (2002), Airaksinen et al. (2012), and our results (Sotero et al., 2015), dexmedetomidine sedation is not sufficient for inducing epileptic activity with short peripheral stimulation. In order to evoke seizures, we had to use long and potent peripheral electrical stimuli (Figures 3, 4 and 5).

To elucidate whether seizures depend on the dexmedetomidine sedation regime, we applied the same stimulation paradigm under a different anesthesia regime, using urethane. Urethane is an anesthetic that produces modest effects on both inhibitory and excitatory systems. The changes exerted on multiple neurotransmitter-gated ion channels are much smaller than those seen with anesthetics more selective for one neurotransmitter system, such as ketamine. Urethane, therefore, is suitable for maintaining anesthesia during electrophysiological recording (Hara and Harris, 2002). Under urethane anesthesia, we did not evoke any seizures. Similarly, Heltovics et al. (1995) applied 3-aminopyridine topically to the surface of cortex and showed that urethane completely abolishes epileptic activity induced by this chemo-convulsant and prevents the development of recurrent seizures. In addition, although kainic acid typically causes convulsions, urethane anesthesia limits the effects of systemic kainic acid application to only electrographic seizures with no convulsions (Saito et al., 2006).

Seizures induced by forepaw stimulation were more frequent than those induced by digit stimulation under similar stimulation parameters. The somatosensory cortical representation of the forepaw is larger than that of individual digits (Waters et al., 1995; Coq and Xerri, 2000; Remple et al., 2003). Therefore, our findings suggest that the vulnerability to seizures increases with the spatial extent of the stimulated cortical tissue.

High frequency oscillations as biomarkers of epileptogenic neural networks

One of the most critical issues for epilepsy is that seizures are nearly unpredictable. A reliable method to detect the seizure state and to localize the discrete epileptogenic zone could enhance the therapeutic possibilities. Indeed, the transition into seizure may not be abrupt and rather, subtle metabolic and/or hemodynamic changes may be informative in predicting seizures and localizing the epileptic zone (Patel et al., 2013). Earlier studies have shown that seizure onset zones can be identified by HFOs (Ochi et al., 2007; Modur et al., 2011; Salami et al., 2014). Our findings demonstrate that LFP changes occur several seconds before the onset of an ictal discharge (Figures 14 and 15). In the rat neocortex, spontaneous, somatosensory-evoked and pathological HFOs include fast ripples (Jones and Barth, 1999; Staba, 2012). As described by Jones and Barth (1999), the sensory-evoked neocortical HFOs occur in conjunction with the biphasic positive-negative somatosensory-evoked potentials. The physiological ripples in humans are seen in all the major regions of the neocortex outside the epileptic zone. In contrast, fast ripples are found at higher

rates only in the epileptic mesial temporal structures (Alkawadri et al., 2014). The pathological HFOs reflect the activity of dysfunctional neural networks that sustain the epileptogenesis (Behr et al., 2014) and can be recorded in the LFP of epileptic patients, (Jacobs et al., 2010; Perucca et al., 2013; Malinowska et al., 2015) as well as in animal epilepsy models (Bragin et al., 2004; Levesque et al., 2011). The power of ripples dramatically increases at the onset as well as during seizures (Grenier et al., 2003; Jiruska et al., 2010). Similarly, our findings show that the power of ripples and fast ripples increases during all somatosensory-evoked epileptic discharges (Figures 14 and 15). Moreover, we show that HFOs recorded in our animals precede all episodes of ictal discharges induced by peripheral somatosensory stimulation. This indicates that the corresponding neural network is more excitable and therefore, more prone to evoke seizures.

A novel artifact-free animal model of reflex seizures: advantages and limitations

We introduce a novel model of somatosensory-evoked reflex seizures that represents brief and artifact-free, non-invasively induced ictal discharges, with no application of either damage or convulsant directly to the brain. Remarkably, even the insertion of intra-cortical probes did not increase the susceptibility of rats to seizure induction (Figure 10). As shown by our optical imaging measurements, the initial epileptic discharges propagate to other cortical regions. Consequently, our model can be used for studying the mechanisms of discharge propagation. The model of seizures we propose is simple to use, does not evoke animal mortality, and does not require sophisticated equipment. Epileptic activity in this animal model is evoked by non-invasive, peripheral somatosensory electrical stimulation. This serves as a more natural way for inducing focal seizures compared to the invasive methods used currently, which involve direct application of drugs to the brain. Electrical stimulation models were the first prototypes introduced for studying seizures, status epilepticus, and neuronal excitability. They are useful for rapid screening of antiepileptic drugs (Loscher, 2011; Reddy and Kuruba, 2013). External electrical stimulation protocols are less harmful to subjects and offer better control of seizures compared to chemical induction methods (Loscher, 2011; Kandratavicius et al., 2014). However, the majority of electrical stimulation methods of seizure induction generate seizures in large parts of the brain, rather than focal seizures. In addition, they cause large artifacts which interfere with electrical recordings and disable investigation of the spatiotemporal mechanisms of seizure induction (Osawa et al., 2013). Our proposed animal model elicits focal seizures that propagate following the

seizure onset. The generation of seizures is artifact-free; therefore, this model can be used to shed light on the characteristics of the onset, propagation, maintenance, and termination of ictal discharges in a lamina-specific manner.

In conclusion, our study reveals that the electrical somatosensory stimulation of rat digits or forepaws provides a novel animal model of somatosensory-evoked reflex seizures for studying therapeutic approaches of human reflex epilepsy. Based on our data, forepaw electrical somatosensory stimulation induces seizures more reliably and at a higher rate than digit stimulation. Therefore, we recommend forepaw stimulation when using this animal model of seizures.

REFERENCES

Adams BE, Kyi M, Reid CA, Myers DE, Xu S, Williams DA, O'Brien TJ (2011) Seizure-like thalamocortical rhythms initiate in the deep layers of the cortex in a co-culture model. Experimental neurology 227:203-209.

Airaksinen AM, Niskanen JP, Chamberlain R, Huttunen JK, Nissinen J, Garwood M, Pitkanen A, Grohn O (2010) Simultaneous fMRI and local field potential measurements during epileptic seizures in medetomidine-sedated rats using raser pulse sequence. Magnetic resonance in medicine 64:1191-1199.

Airaksinen AM, Hekmatyar SK, Jerome N, Niskanen JP, Huttunen JK, Pitkanen A, Kauppinen RA, Grohn OH (2012) Simultaneous BOLD fMRI and local field potential measurements during kainic acid-induced seizures. Epilepsia 53:1245-1253.

Alkawadri R, Gaspard N, Goncharova, II, Spencer DD, Gerrard JL, Zaveri H, Duckrow RB, Blumenfeld H, Hirsch LJ (2014) The spatial and signal characteristics of physiologic high frequency oscillations. Epilepsia 55:1986-1995.

Annegers JF, Coan SP (2000) The risks of epilepsy after traumatic brain injury. Seizure 9:453-457.

Arican P, Dundar NO, Cavusoglu D, Ozdemir TR, Gencpinar P (2017) Somatosensory reflex seizures in a child with epilepsy related to novel SCN1A mutation. Child's nervous system : ChNS : official journal of the International Society for Pediatric Neurosurgery 33:677-680.

Bahar S, Suh M, Zhao M, Schwartz TH (2006) Intrinsic optical signal imaging of neocortical seizures: the 'epileptic dip'. Neuroreport 17:499-503.

Barkai E, Friedman A, Grossman Y, Gutnick MJ (1995) Laminar pattern of synaptic inhibition during convulsive activity induced by 4-aminopyridine in neocortical slices. Journal of neurophysiology 73:1462-1467.

Barnes SJ, Pinel JP (2001) Conditioned effects of kindling. Neuroscience and biobehavioral reviews 25:745-751.

Behr C, D'Antuono M, Hamidi S, Herrington R, Levesque M, Salami P, Shiri Z, Kohling R, Avoli M (2014) Limbic networks and epileptiform synchronization: the view from the experimental side. International review of neurobiology 114:63-87.

Bekker A, Sturaitis MK (2005) Dexmedetomidine for neurological surgery. Neurosurgery 57:1-10; discussion 11-10.
Benkovic SA, O'Callaghan JP, Miller DB (2006) Regional neuropathology following kainic acid intoxication in adult and aged C57BL/6J mice. Brain research 1070:215-231.
Blume WT, Jones DC, Pathak P (2004) Properties of after-discharges from cortical electrical stimulation in focal epilepsies. Clinical neurophysiology : official journal of the International Federation of Clinical Neurophysiology 115:982-989.
Bokil H, Andrews P, Kulkarni JE, Mehta S, Mitra PP (2010) Chronux: a platform for analyzing neural signals. Journal of neuroscience methods 192:146-151.
Borbely S, Halasy K, Somogyvari Z, Detari L, Vilagi I (2006) Laminar analysis of initiation and spread of epileptiform discharges in three in vitro models. Brain research bulletin 69:161-167.
Boucetta S, Chauvette S, Bazhenov M, Timofeev I (2008) Focal generation of paroxysmal fast runs during electrographic seizures. Epilepsia 49:1925-1940.
Bragin A, Wilson CL, Almajano J, Mody I, Engel J, Jr. (2004) High-frequency oscillations after status epilepticus: epileptogenesis and seizure genesis. Epilepsia 45:1017-1023.
Cavanaugh JR, Bair W, Movshon JA (2002) Nature and interaction of signals from the receptive field center and surround in macaque V1 neurons. Journal of neurophysiology 88:2530-2546.
Chauvette S, Soltani S, Seigneur J, Timofeev I (2016) In vivo models of cortical acquired epilepsy. Journal of neuroscience methods 260:185-201.
Chen JW, O'Farrell AM, Toga AW (2000) Optical intrinsic signal imaging in a rodent seizure model. Neurology 55:312-315.
Coq JO, Xerri C (2000) Age-related alteration of the forepaw representation in the rat primary somatosensory cortex. Neuroscience 99:403-411.
Curia G, Eastman CL, Miller JW, D'Ambrosio R (2016) Modeling Post-Traumatic Epilepsy for Therapy Development. In: Translational Research in Traumatic Brain Injury (Laskowitz D, Grant G, eds). Boca Raton (FL): CRC Press/Taylor and Francis Group.
Dawson R, Jr., Wallace DR (1992) Kainic acid-induced seizures in aged rats: neurochemical correlates. Brain research bulletin 29:459-468.
Deonna T (1998) Reflex seizures with somatosensory precipitation. Clinical and electroencephalographic patterns and differential diagnosis, with emphasis on reflex myoclonic epilepsy of infancy. Advances in neurology 75:193-206.
Derdikman D, Hildesheim R, Ahissar E, Arieli A, Grinvald A (2003) Imaging spatiotemporal dynamics of surround inhibition in the barrels somatosensory cortex. The Journal of neuroscience : the official journal of the Society for Neuroscience 23:3100-3105.
Dorn T, Witte OW (1995) Refractory periods following interictal spikes in acute experimentally induced epileptic foci. Electroencephalography and clinical neurophysiology 94:80-85.
Engel J, Jr. (2004) Models of focal epilepsy. Supplements to Clinical neurophysiology 57:392-399.
Engel J, Jr., Kuhl DE, Phelps ME (1982) Patterns of human local cerebral glucose metabolism during epileptic seizures. Science (New York, NY) 218:64-66.
Flynn C, Young NA, Teskey GC (2010) Seizures, but not lowered seizure thresholds, results in larger neocortical motor maps and concomitant disruptions in skilled motor behaviour. Behavioural brain research 214:60-65.
Franceschini MA, Radhakrishnan H, Thakur K, Wu W, Ruvinskaya S, Carp S, Boas DA (2010) The effect of different anesthetics on neurovascular coupling. NeuroImage 51:1367-1377.

Freeman J, Nicholson C (1975) Experimental optimization of current source-density technique for anuran cerebellum. Journal of Neurophysiology 38:369-382.

Fukuda M, Vazquez AL, Zong X, Kim SG (2013) Effects of the alpha(2)-adrenergic receptor agonist dexmedetomidine on neural, vascular and BOLD fMRI responses in the somatosensory cortex. The European journal of neuroscience 37:80-95.

Gerlach AT, Dasta JF (2007) Dexmedetomidine: an updated review. Ann Pharmacother 41:245-252.

Gertler R, Brown HC, Mitchell DH, Silvius EN (2001) Dexmedetomidine: a novel sedative-analgesic agent. Proc (Bayl Univ Med Cent) 14:13-21.

Goddard GV, McIntyre DC, Leech CK (1969) A permanent change in brain function resulting from daily electrical stimulation. Experimental neurology 25:295-330.

Gorter JA, van Vliet EA, Lopes da Silva FH (2016) Which insights have we gained from the kindling and post-status epilepticus models? Journal of neuroscience methods 260:96-108.

Grenier F, Timofeev I, Steriade M (2003) Neocortical very fast oscillations (ripples, 80-200 Hz) during seizures: intracellular correlates. Journal of neurophysiology 89:841-852.

Grinvald A, Shoham D, Shmuel A, Glaser D, Vanzetta I, Shtoyerman E, Slovin H, Sterkin A, Wijnbergen C, Hildesheim R (1999) Modern techniques in neuroscience research. In-vivo Optical Imaging of cortical Architecture and Dynamics Springer:893.

Grover EH, Nazzal Y, Hirsch LJ (2016) Treatment of Convulsive Status Epilepticus. Current treatment options in neurology 18:11.

Guerrini R, Genton P, Dravet C, Viallat D, Bureau M, Horton EJ, Roger J (1992) Compulsive somatosensory self-stimulation inducing epileptic seizures. Epilepsia 33:509-516.

Haglund MM, Hochman DW (2007) Imaging of intrinsic optical signals in primate cortex during epileptiform activity. Epilepsia 48 Suppl 4:65-74.

Hara K, Harris RA (2002) The anesthetic mechanism of urethane: the effects on neurotransmitter-gated ion channels. Anesthesia and analgesia 94:313-318, table of contents.

Harris S, Boorman L, Bruyns-Haylett M, Kennerley A, Ma H, Zhao M, Overton PG, Schwartz TH, Berwick J (2014) Contralateral dissociation between neural activity and cerebral blood volume during recurrent acute focal neocortical seizures. Epilepsia 55:1423-1430.

Harris SS, Boorman LW, Kennerley AJ, Sharp PS, Martin C, Redgrave P, Schwartz TH, Berwick J (2018) Seizure epicenter depth and translaminar field potential synchrony underlie complex variations in tissue oxygenation during ictal initiation. NeuroImage 171:165-175.

Hattiangady B, Kuruba R, Shetty AK (2011) Acute Seizures in Old Age Leads to a Greater Loss of CA1 Pyramidal Neurons, an Increased Propensity for Developing Chronic TLE and a Severe Cognitive Dysfunction. Aging and disease 2:1-17.

Heltovics G, Boda B, Szente M (1995) Anticonvulsive effect of urethane on aminopyridine-induced epileptiform activity. Neuroreport 6:577-580.

Hsieh CY, Chiou NJ, Wu YJ, Tsai JJ, Huang CW (2011) Somatosensory rub evoked reflex epilepsy of a temporal lobe origin. Neurological sciences : official journal of the Italian Neurological Society and of the Italian Society of Clinical Neurophysiology 32:297-299.

Italiano D, Ferlazzo E, Gasparini S, Spina E, Mondello S, Labate A, Gambardella A, Aguglia U (2014) Generalized versus partial reflex seizures: A review. Seizure 23:512-520.

Italiano D, Striano P, Russo E, Leo A, Spina E, Zara F, Striano S, Gambardella A, Labate A, Gasparini S, Lamberti M, De Sarro G, Aguglia U, Ferlazzo E (2016) Genetics of reflex seizures and epilepsies in humans and animals. Epilepsy research 121:47-54.

Jacobs J, Levan P, Chatillon CE, Olivier A, Dubeau F, Gotman J (2009) High frequency oscillations in intracranial EEGs mark epileptogenicity rather than lesion type. Brain : a journal of neurology 132:1022-1037.

Jacobs J, Zijlmans M, Zelmann R, Olivier A, Hall J, Gotman J, Dubeau F (2010) Value of electrical stimulation and high frequency oscillations (80-500 Hz) in identifying epileptogenic areas during intracranial EEG recordings. Epilepsia 51:573-582.

Jefferys JG, Menendez de la Prida L, Wendling F, Bragin A, Avoli M, Timofeev I, Lopes da Silva FH (2012) Mechanisms of physiological and epileptic HFO generation. Progress in neurobiology 98:250-264.

Jiruska P, Powell AD, Chang WC, Jefferys JG (2010) Electrographic high-frequency activity and epilepsy. Epilepsy research 89:60-65.

Jones MS, Barth DS (1999) Spatiotemporal organization of fast (>200 Hz) electrical oscillations in rat Vibrissa/Barrel cortex. Journal of neurophysiology 82:1599-1609.

Kalamangalam GP, Tandon N, Slater JD (2014) Dynamic mechanisms underlying afterdischarge: a human subdural recording study. Clinical neurophysiology : official journal of the International Federation of Clinical Neurophysiology 125:1324-1338.

Kandratavicius L, Balista PA, Lopes-Aguiar C, Ruggiero RN, Umeoka EH, Garcia-Cairasco N, Bueno-Junior LS, Leite JP (2014) Animal models of epilepsy: use and limitations. Neuropsychiatric disease and treatment 10:1693-1705.

Kanemoto K, Watanabe Y, Tsuji T, Fukami M, Kawasaki J (2001) Rub epilepsy: a somatosensory evoked reflex epilepsy induced by prolonged cutaneous stimulation. Journal of neurology, neurosurgery, and psychiatry 70:541-543.

Kharatishvili I, Pitkanen A (2010) Association of the severity of cortical damage with the occurrence of spontaneous seizures and hyperexcitability in an animal model of posttraumatic epilepsy. Epilepsy research 90:47-59.

Koepp MJ, Caciagli L, Pressler RM, Lehnertz K, Beniczky S (2016) Reflex seizures, traits, and epilepsies: from physiology to pathology. The Lancet Neurology 15:92-105.

Lauritzen M, Gold L (2003) Brain function and neurophysiological correlates of signals used in functional neuroimaging. The Journal of neuroscience : the official journal of the Society for Neuroscience 23:3972-3980.

Lesser RP, Lee HW, Webber WR, Prince B, Crone NE, Miglioretti DL (2008) Short-term variations in response distribution to cortical stimulation. Brain : a journal of neurology 131:1528-1539.

Lesser RP, Kim SH, Beyderman L, Miglioretti DL, Webber WR, Bare M, Cysyk B, Krauss G, Gordon B (1999) Brief bursts of pulse stimulation terminate afterdischarges caused by cortical stimulation. Neurology 53:2073-2081.

Levesque M, Bortel A, Gotman J, Avoli M (2011) High-frequency (80-500 Hz) oscillations and epileptogenesis in temporal lobe epilepsy. Neurobiology of disease 42:231-241.

Li L, Kriukova K, Engel J, Jr., Bragin A (2018) Seizure development in the acute intrahippocampal epileptic focus. Scientific reports 8:1423.

Loscher W (1999) Animal Models of Epilepsy and Epileptic Seizures. In: Antiepileptic Drugs Pharmacology and Therapeutics (Eadie MI, Vajda FIE, eds), pp 19-62. Berlin Heidelberg: Springer-Verlag.

Loscher W (2011) Critical review of current animal models of seizures and epilepsy used in the discovery and development of new antiepileptic drugs. Seizure 20:359-368.

Loscher W (2017a) Animal Models of Seizures and Epilepsy: Past, Present, and Future Role for the Discovery of Antiseizure Drugs. Neurochemical research 42:1873-1888.

Loscher W (2017b) The Search for New Screening Models of Pharmacoresistant Epilepsy: Is Induction of Acute Seizures in Epileptic Rodents a Suitable Approach? Neurochemical research 42:1926-1938.

Lothman EW (1996) Neurobiology as a basis for rational polypharmacy. Section overview for rational polypharmacy conference. Epilepsy research Supplement 11:3-7.

Ma H, Zhao M, Schwartz TH (2013) Dynamic neurovascular coupling and uncoupling during ictal onset, propagation, and termination revealed by simultaneous in vivo optical imaging of neural activity and local blood volume. Cerebral cortex (New York, NY : 1991) 23:885-899.

Malinowska U, Bergey GK, Harezlak J, Jouny CC (2015) Identification of seizure onset zone and preictal state based on characteristics of high frequency oscillations. Clinical neurophysiology : official journal of the International Federation of Clinical Neurophysiology 126:1505-1513.

Marks DA, Kim J, Spencer DD, Spencer SS (1995) Seizure localization and pathology following head injury in patients with uncontrolled epilepsy. Neurology 45:2051-2057.

Meeren HK, Pijn JP, Van Luijtelaar EL, Coenen AM, Lopes da Silva FH (2002) Cortical focus drives widespread corticothalamic networks during spontaneous absence seizures in rats. The Journal of neuroscience : the official journal of the Society for Neuroscience 22:1480-1495.

Migani P, Magnone MC, Rossolini G, Piantanelli L (2000) Excitatory amino acid receptors in the prefrontal cortex of aging mice. Neurobiology of aging 21:607-612.

Modur PN, Zhang S, Vitaz TW (2011) Ictal high-frequency oscillations in neocortical epilepsy: implications for seizure localization and surgical resection. Epilepsia 52:1792-1801.

Morimoto K, Mason SE, Goddard GV (1987) Kindling-induced changes in the EEG recorded during stimulation from the site of stimulation. II. Comparison between spontaneous and evoked potentials. Experimental neurology 97:1-16.

Murthy VN, Fetz EE (1996) Synchronization of neurons during local field potential oscillations in sensorimotor cortex of awake monkeys. Journal of neurophysiology 76:3968-3982.

Ochi A, Otsubo H, Donner EJ, Elliott I, Iwata R, Funaki T, Akizuki Y, Akiyama T, Imai K, Rutka JT, Snead OC, 3rd (2007) Dynamic changes of ictal high-frequency oscillations in neocortical epilepsy: using multiple band frequency analysis. Epilepsia 48:286-296.

Oishi R, Suenaga N (1982) The role of the locus coeruleus in regulation of seizure susceptibility in rats. Japanese journal of pharmacology 32:1075-1081.

Osawa S, Iwasaki M, Hosaka R, Matsuzaka Y, Tomita H, Ishizuka T, Sugano E, Okumura E, Yawo H, Nakasato N, Tominaga T, Mushiake H (2013) Optogenetically induced seizure and the longitudinal hippocampal network dynamics. PloS one 8:e60928.

Ozen LJ, Young NA, Koshimori Y, Teskey GC (2008) Low-frequency stimulation reverses kindling-induced neocortical motor map expansion. Neuroscience 153:300-307.

Panayiotopoulos CP (2005) Reflex Seizures and Reflex Epilepsies. In: The Epilepsies: Seizures, Syndromes and Management (Panayiotopoulos CP, ed). Oxfordshire (UK): Bladon Medical Publishing.

Patel KS, Zhao M, Ma H, Schwartz TH (2013) Imaging preictal hemodynamic changes in neocortical epilepsy. Neurosurgical focus 34:E10.

Paxinos G, Watson C (2005) The rat brain in stereotaxic coordinates., 5th Edition. Boston: Elsevier Academic Press.

Perucca P, Dubeau F, Gotman J (2013) Widespread EEG changes precede focal seizures. PloS one 8:e80972.

Quiroga RQ, Nadasdy Z, Ben-Shaul Y (2004) Unsupervised spike detection and sorting with wavelets and superparamagnetic clustering. Neural computation 16:1661-1687.

Racine RJ (1975) Modification of seizure activity by electrical stimulation: cortical areas. Electroencephalography and clinical neurophysiology 38:1-12.

Reddy DS, Kuruba R (2013) Experimental models of status epilepticus and neuronal injury for evaluation of therapeutic interventions. International journal of molecular sciences 14:18284-18318.

Remple MS, Henry EC, Catania KC (2003) Organization of somatosensory cortex in the laboratory rat (Rattus norvegicus): Evidence for two lateral areas joined at the representation of the teeth. The Journal of comparative neurology 467:105-118.

Revilla V, Robles MS, Bermejo JC, Paniagua MA, Fernandez-Lopez A (1999) Seizure-refractory period after a single stimulation and inhibition of seizures after repetitive stimulation in the gerbil: effects on blood cortisol levels. Epilepsia 40:1-4.

Saito T, Sakamoto K, Koizumi K, Stewart M (2006) Repeatable focal seizure suppression: a rat preparation to study consequences of seizure activity based on urethane anesthesia and reversible carotid artery occlusion. Journal of neuroscience methods 155:241-250.

Sala-Padro J, Toledo M, Sarria S, Santamarina E, Gonzalez-Cuevas M, Sueiras-Gil M, Salas-Puig J (2015) Reflex seizures triggered by cutaneous stimuli. Seizure 33:72-75.

Salami P, Levesque M, Benini R, Behr C, Gotman J, Avoli M (2014) Dynamics of interictal spikes and high-frequency oscillations during epileptogenesis in temporal lobe epilepsy. Neurobiology of disease 67:97-106.

Sarkisian MR (2001) Overview of the Current Animal Models for Human Seizure and Epileptic Disorders. Epilepsy & behavior : E&B 2:201-216.

Schwartz TH, Bonhoeffer T (2001) In vivo optical mapping of epileptic foci and surround inhibition in ferret cerebral cortex. Nature medicine 7:1063-1067.

Shariff S, Suh M, Zhao M, Ma H, Schwartz TH (2006) Recent developments in oximetry and perfusion-based mapping techniques and their role in the surgical treatment of neocortical epilepsy. Epilepsy & behavior : E&B 8:363-375.

Sotero RC, Bortel A, Naaman S, Mocanu VM, Kropf P, Villeneuve MY, Shmuel A (2015) Laminar Distribution of Phase-Amplitude Coupling of Spontaneous Current Sources and Sinks. Frontiers in neuroscience 9:454.

Sperber EF, Veliskova J, Germano IM, Friedman LK, Moshe SL (1999) Age-dependent vulnerability to seizures. Advances in neurology 79:161-169.

Staba RJ (2012) Normal and Pathologic High-Frequency Oscillations. In: Jasper's Basic Mechanisms of the Epilepsies (Noebels JL, Avoli M, Rogawski MA, Olsen RW, Delgado-Escueta AV, eds). Bethesda (MD): National Center for Biotechnology Information (US).

Striano S, Meo R, Bilo L, Ruosi P (1992) Partial self induced seizures: an uncommon motivation for auto-induction. Journal of neurology, neurosurgery, and psychiatry 55:74-75.

Striano S, Coppola A, del Gaudio L, Striano P (2012) Reflex seizures and reflex epilepsies: old models for understanding mechanisms of epileptogenesis. Epilepsy research 100:1-11.

Suh M, Bahar S, Mehta AD, Schwartz TH (2005) Temporal dependence in uncoupling of blood volume and oxygenation during interictal epileptiform events in rat neocortex. The Journal of neuroscience : the official journal of the Society for Neuroscience 25:68-77.

Suzuki S, Sassa K, Abe Y, Yamanouchi H (2015) Generalized seizure with falling and unresponsive staring provoked by somatosensory stimulation: a video-EEG study. Epileptic disorders : international epilepsy journal with videotape 17:336-339.

Timofeev I, Steriade M (2004) Neocortical seizures: initiation, development and cessation. Neuroscience 123:299-336.

Timofeev I, Chauvette S, Soltani S (2014) Neocortical focus: experimental view. International review of neurobiology 114:9-33.

Vaknin G, DiScenna P, Teyler T (1988) A method for calculating current source density (CSD) analysis without resorting to recording sites outside the sampling volume. Journal of neuroscience methods 24:131-135.

van Vliet EA, Gorter JA (2017) Electrical Stimulation Seizure Models. In: Models of Seizures and Epilepsy (Second Edition) (Pitkänen A, Buckmaster PS, Galanopoulou AS, Moshé SL, eds), pp 474-488: Academic Press.

Vuong J, Henderson AK, Tuor UI, Dunn JF, Teskey GC (2011) Persistent enhancement of functional MRI responsiveness to sensory stimulation following repeated seizures. Epilepsia 52:2285-2292.

Waters RS, Li CX, McCandlish CA (1995) Relationship between the organization of the forepaw barrel subfield and the representation of the forepaw in layer IV of rat somatosensory cortex. Experimental brain research 103:183-197.

Wendling F, Bartolomei F, Bellanger JJ, Chauvel P (2002) Epileptic fast activity can be explained by a model of impaired GABAergic dendritic inhibition. The European journal of neuroscience 15:1499-1508.

Whittington RA, Virag L, Vulliemoz Y, Cooper TB, Morishima HO (2002) Dexmedetomidine increases the cocaine seizure threshold in rats. Anesthesiology 97:693-700.

Wolf P (2015) Reflex epileptic mechanisms in humans: Lessons about natural ictogenesis. Epilepsy & behavior : E&B.

Yang L, Benardo LS (1998) Removal of superficial inhibition releases hyperexcitability in middle and deep horizontal slices from rat somatosensory neocortex. Neuroscience letters 257:33-36.

Yang L, Benardo LS (2002) Laminar properties of 4-aminopyridine-induced synchronous network activities in rat neocortex. Neuroscience 111:303-313.

Zhang XM, Zhu SW, Duan RS, Mohammed AH, Winblad B, Zhu J (2008) Gender differences in susceptibility to kainic acid-induced neurodegeneration in aged C57BL/6 mice. Neurotoxicology 29:406-412.

Zhao M, Ma H, Suh M, Schwartz TH (2009) Spatiotemporal dynamics of perfusion and oximetry during ictal discharges in the rat neocortex. The Journal of neuroscience : the official journal of the Society for Neuroscience 29:2814-2823.